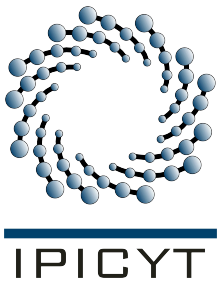

INSTITUTO POTOSINO DE INVESTIGACIÓN CIENTÍFICA Y TECNOLÓGICA, A.C.

POSGRADO EN CONTROL Y SISTEMAS DINÁMICOS

Fractional Order Chaotic Systems and Their Electronic Design

Tesis que presenta

Ernesto Zambrano Serrano

Para obtener el grado de

Doctor en Control y Sistemas Dinámicos

Codirectores de la Tesis:

Dr. Eric Campos Cantón (IPICyT)

Dr. Jesús Manuel Muñoz Pacheco (FCE-BUAP)

San Luis Potosí, S.L.P., Julio 2017

IPICYT

Constancia de aprobación de la tesis

La tesis **"Fractional Order Chaotic Systems and Their Electronic Design"** presentada para obtener el Grado de Doctor en Control y Sistemas Dinámicos fue elaborada por **Ernesto Zambrano Serrano** y aprobada el **siete de julio del dos mil diecisiete** por los suscritos, designados por el Colegio de Profesores de la División de Matemáticas Aplicadas del Instituto Potosino de Investigación Científica y Tecnológica, A.C.

Dr. Eric Campos Cantón
Codirector de Tesis

Dr. Jesús Manuel Muñoz Pacheco
Codirector de Tesis

Dr. Diego Langarica Córdoba
Jurado en el Examen

Dr. Juan Gonzalo Barajas Ramírez
Jurado en el Examen

Dr. Javier Salvador González Salas
Jurado en el Examen

Créditos Institucionales

Esta tesis fue elaborada en la División de Matemáticas Aplicadas del Instituto Potosino de Investigación Científica y Tecnológica, A.C., bajo la codirección de los Doctores Eric Campos Cantón y Jesús Manuel Muñoz Pacheco.

Durante la realización del trabajo el autor recibió una beca académica del Consejo Nacional de Ciencia y Tecnología No. de registro 237152 y del Instituto Potosino de Investigación Científica y Tecnológica, A. C.

IPICYT

Instituto Potosino de Investigación Científica y Tecnológica, A.C.

Acta de Examen de Grado

El Secretario Académico del Instituto Potosino de Investigación Científica y Tecnológica, A.C., certifica que en el Acta 001 del Libro Primero de Actas de Exámenes de Grado del Programa de Doctorado en Control y Sistemas Dinámicos está asentado lo siguiente:

En la ciudad de San Luis Potosí a los 7 días del mes de julio del año 2017, se reunió a las 15:00 horas en las instalaciones del Instituto Potosino de Investigación Científica y Tecnológica, A.C., el Jurado integrado por:

Dr. Juan Gonzalo Barajas Ramírez	**Presidente**	**IPICYT**
Dr. Jesús Manuel Muñoz Pacheco	**Secretario**	**BUAP**
Dr. Diego Langarica Córdoba	**Sinodal**	**IPICYT**
Dr. Eric Campos Cantón	**Sinodal**	**IPICYT**
Dr. Javier Salvador González Salas	**Sinodal externo**	**UPSLP**

a fin de efectuar el examen, que para obtener el Grado de:

DOCTOR EN CONTROL Y SISTEMAS DINÁMICOS

sustentó el C.

Ernesto Zambrano Serrano

sobre la Tesis intitulada:

Fractional Order Chaotic Systems and Their Electronic Design

que se desarrolló bajo la dirección de

Dr. Eric Campos Cantón
Dr. Jesús Manuel Muñoz Pacheco (BUAP)

El Jurado, después de deliberar, determinó

APROBARLO

Dándose por terminado el acto a las 17:00 horas, procediendo a la firma del Acta los integrantes del Jurado. Dando fe el Secretario Académico del Instituto.

A petición del interesado y para los fines que al mismo convengan, se extiende el presente documento en la ciudad de San Luis Potosí, S.L.P., México, a los 7 días del mes de julio de 2017.

Dr. Horacio Flores Zúñiga
Secretario Académico

Mtra. Ivonne Lizette Cuevas Vélez
Jefa del Departamento del Posgrado

INSTITUTO POTOSINO DE INVESTIGACIÓN CIENTÍFICA Y TECNOLÓGICA, A.C.
IPICYT
SECRETARIA ACADEMICA

Dedicated to my family
for keeping my chaotic life in order.

Acknowledgement

I want to express my gratitude to the people who have helped in the successful completion of this dissertation. First, I would like to thank my parents, Mario Zambrano and Lupita Serrano for their support with their interest in my education while growing up and over the subsequent years. To whom, with much affection, I dedicate the effort printed on each page of this thesis. Without forgetting Mario, Estefania and Adrianita, this is for you, for supporting me spiritually throughout writing this thesis and my life in general

I would also like to thank my gratitude to my advisors Dr. Eric Campos and Dr. Jesús Muñoz for your guidance throughout this process, for the continuous support of my Ph.D study and related research, for your patience, motivation, and immense knowledge. Your guidance helped me in all the time of research and writing of this thesis. I cannot thank enough their great support motivation and help. I deeply appreciate your friendship.

I would like to thank the rest of my thesis committee: Dr. Juan Gonzalo Barajas Ramírez, Dr. Diego Langarica Córdoba and Dr. Javier Salvador González Salas, for their insightful comments and encouragement, but also for the hard question which incentivized me to widen my research from various perspectives.

The people at IPICyT and FCE-BUAP, for making those great and interesting places to develop the research. Those people have contributed immensely to my personal and professional time. The institutions have been a source of friendships as well as good advice and collaboration.

This thesis was partially supported by CONACYT through Project No. 258880 (Proyecto Apoyado por el Fondo Sectorial de Investigación para la Educación).

Contents

List of Figures

List of symbols

$< (>)$ Less (greater) than

$\approx$ Approximately equal

$\arg$ Argument of complex number

$\square$ Designation of the end of proofs

$\cup$ Union of sets

$\equiv$ Equivalent to

$\forall$ For all

$\Gamma(\cdot)$ Euler's gamma function

$\in$ Belongs to

$\leq (\geq)$ Less (greater) than or equal to

$\lim$ Limit

$\mathbb{R}$ The set of real numbers

$\mathbb{R}^{m \times n}$ The set of all $m \times n$ matrices with elements in $\mathbb{R}$

$\max$ Maximum

$\min$	Minimun
$\neq$	Not equal to
$\rightarrow$	Tends to
$\subset$	Subset of
$\sum$	Summation
$\sup$	Supremum, the least upper bound
$\{\cdot\}$	Set
${}_aD_t^\alpha$	Fractional order derivative/integral operator
A^T	The transpose of a matrix obtained by interchanging the rows and columns of A
$E*$	Equilibrium point
$E_{\alpha,\beta}$	Mittag-Leffler function
$f : S_1 \rightarrow S_2$	A function f mapping a set S_1 into a set S_2
$L\{\cdot\}$	Laplace transform
FC	Fractional Calculus
FOUDS	Fractional Order Unstable Dissipative System
GL	Grünwald-Letnikov definition
LLE	Largest Lyapunov Exponen
LTI	Linear Time Invariant
UDS	Unstable Dissipative System

Resumen

Con el desarrollo del cálculo fraccionario y la teoría del caos, los sistemas caóticos de orden fraccionario se han convertido en una forma útil de evaluar las características de los sistemas dinámicos. En esta dirección, esta tesis es principalmente relacionada, es decir, en el estudio de sistemas caóticos de orden fraccionario, basado en sistemas disipativos de inestables, un sistema disipativo de inestable de orden fraccionario es propuesto. Algunas propiedades dinámicas como puntos de equilibrio, exponentes de Lyapunov, diagramas de bifurcación y comportamientos dinámicos caóticos del sistema caótico de orden fraccionario son estudiados. Los resultados obtenidos muestran claramente que el sistema discutido presenta un comportamiento caótico. Por medio de considerar la teoría del cálculo fraccionario y simulaciones numéricas, se muestra que el comportamiento caótico existe en el sistema de tres ecuaciones diferenciales de orden fraccionario acopladas, con un orden menor a tres. Estos resultados son validados por la existencia de un exponente positivo de Lyapunov, además de algunos diagramas de fase. Por otra parte, la presencia de caos es también verificada obteniendo la herradura topológica. Dicha prueba topológica garantiza la generaciń de caos en el sistema de orden fraccionario propuesto. En orden de verificar la efectividad del sistema propuesto, un circuito electrónico es diseñado con el fin de sintetizar el sistema caótico de orden fraccionario.

Abstract

With the development of fractional order calculus and chaos theory, the fractional order chaotic systems have become a useful way to evaluate characteristics of dynamical systems and forecast the trend of complex systems. In this direction, this thesis is primarily concerned with the study of fractional order chaotic systems, based on an unstable dissipative system (UDS), a fractional order unstable dissipative system (FOUDS) is proposed. Dynamical properties, such as equilibrium points, Lyapunov exponents, bifurcation diagrams and phase diagrams of the fractional order chaotic system are studied. The obtained results shown that the fractional order unstable dissipative system has a chaotic behavior. By utilizing the fractional calculus theory and computer simulations, it is found that chaos exists in the fractional order three dimensional system with order less than three. The lowest order to yield chaos in this system is 2.4. The results are validated by the existence of one positive Lyapunov exponent, phase diagrams; Besides, the presence of chaos is also verified obtaining the topological horseshoe. That topological proof guarantees the chaos generation in the proposed fractional order unstable dissipative system. In order to verify the effectiveness of the proposed system, an electronic circuit is designed with the purpose of synthesize the fractional order chaotic system, the fractional order integral is realized with electronic circuit utilizing the synthesis of a fractance circuit. The realization has been done via synthesis as passive RC circuits connected to an operational amplifier. The continuos fractional expansion have been utilized on fractional integration transfer function which has been approximated to integer order rational transfer func-

tion considering the Charef Method. The analogue electronics circuits have been simulated using HSPICE.

Introduction

The concept of differentiation and integration to noninteger order is by no means new. In 1695 L'Hôpital sent a letter to Leibniz, in his letter, a question about the order the derivatives emerged: what meaning could be ascribed to derivative of order n if n was a fraction? In a forecast answer, Leibniz predicted the beginning of the area that today is named fractional calculus (FC). In fact, FC has attracted the attention of many famous mathematicians. It was Euler (1738) that observed the problem for a derivative of noninteger order, he noted that the result of the evaluation of a derivative of a power function has a meaning for noninteger orders [1]. Laplace (1812) suggested the idea of differentiation of noninteger order for functions representable by an integral [1]. Fourier (1822) proposed an integral representation in order to define the derivative, this version is considered the first definition for the derivative of fractional (positive) order [2]. Abel (1826) applied the fractional calculus in the solution of an integral equation that arises in the formulation of the tautochrone problem, which is considered to be the first application of FC [2, 3]. Liouville (1832) suggested a definition based on the formula for differentiating the exponential function, which is known as his first definition [3, 4]. The second definition given by Liouville is presented in terms of an integral which is the integration of noninteger order [3–5].

It was Grünwald and Letnikov who first unified the results of Liouville and Riemann, they develop a method to noninteger order derivatives in terms of a convergent series. But it was not until 1900 that the theory about FC has a great interest, and in an attempt to formulate particular problems, other definitions were pro-

posed that gave a point of departure for the development of this area. Caputo (1967) proposed a definition to discuss problems involving a fractional differential equation with initial conditions [1–5]. The definition given by Caputo inverts the position of integral and derivative operators with the noninteger order derivative in relation to Riemann-Liouville definition [6]. The main difference between Caputo and Riemann-Liouville definitions is that the first calculate derivative of integer order and after calculate the integral of noninteger order. In the definition of Riemann-Liouville calculate the integral of noninteger order and after calculate the derivative of integer order [1–6]. Also, it can be demonstrated that both definitions become equivalent under the same homogeneous initial conditions [7].

The theory had been extended to include fractional order derivative operators D^m, where m could be rational, irrational, complex or real. Thus it is important to remark that the name fractional calculus is improperly used words. A more accurate description should be differentiation and integration to an arbitrary order. However, there are a lot of works in the literature that use fractional more generally to refer to the same concept. For this reason, this thesis adhere to tradition and refer to be consistent as fractional calculus.

Recently, studying fractional order systems has become an active research area [8–14]. The fractional order models give more accuracy results than the corresponding integer-order models [15–17]. There are two main features of that claim; the fractional order parameter improves the system performance by increasing one degree of freedom, and the other one is related to fractional derivatives provides a valuable instrument for the description of memory and hereditary properties in various processes [15–18]. Therefore, the fractional derivatives have been used to describe elegantly interdisciplinary applications; for instance, in [14] the projectile motion is examined by means of fractional calculus, concluding that the launching angle that maximizes the horizontal range is a function of the arbitrary order of the fractional derivative; in [19] a fractional order model of tumor cells growth and their interaction with general immune effector cells is studied; a generalization for the stability analysis of neutral fractional-delay system. Where

the stability can be evaluated by calculating by the number of the unstable characteristic roots is presented in [20]; in control theory a fractional order controller has been reported in some applications such as backlash vibration suppression control of torsional systems [21]; in viscoelastic materials, the fractional order damping element provides a superior model because it is modeled as a force proportional to the fractional order derivative of the displacement [22]; in image processing a fractional differential algorithm could preserve the information of weak texture, while enhancing the edge of image [23]; also in dielectric polarization a fractional model is better to study the relation between the dynamic polarization, frequency and electric field amplitude [24]; and so on [25, 26].

Fractional integrals and derivatives also appears in theory of chaotic systems. One of the main objectives in the literature is found that chaotic behavior in fractional order systems. Usually chaotic attractors cannot be observed in continuous nonlinear systems whose order is less than three, so it is highly interesting to analyze the routes to get chaos of fractional order systems with low orders. The fractional derivatives have complex geometrical interpretation due of their nonlocal character and high nonlinearity; the power spectrum of fractional order chaotic systems fluctuates complexly increasing the chaoticity in frequency domain; and the computational complexity goal is also achieved. More specifically, the security in cryptosystems based on chaos can be increased using the derivative orders of fractional chaotic systems as secret keys in addition to the system's parameters [25]; so, the complexity of the verification of each key is strengthened causing the traditional cracking algorithms of chaotic masking to be unusable. Therefore, new fractional chaotic systems are crucial to enhance the performance of several integer-order chaos-based applications. Recently, engineering applications using fractional order chaotic systems have been demonstrated, such as a digital cryptography approach, an image encryption method, a cipher and an authenticated encryption scheme [26].

The objective of this thesis is mainly targeted towards the fractional order nonlinear dynamical systems. The objective is to propose a fractional order unstable dissipative system considering the dynamical characteristics of the unstable dis-

sipative system. In a first instance, analyze the effects related to its dynamics of the fractional order unstable dissipative system i.e., finding an effective minimum order using the same system's parameters as integer order version while chaos behavior is preserved. The chaotic attractor of the fractional system appears as a result of the combination of several unstable one-spiral trajectories around a saddle hyperbolic equilibrium point. The resulting chaotic attractor from the fractional order dynamical systems has the same number of equilibria as scrolls as shown herein. The fractional order unstable dissipative system is solved by means of the improved version of Adams-Bashforth-Moulton numerical algorithm and the chaotic attractor can be observed for different orders. In addition, based on topological horseshoe analysis method, a topological horseshoe is found in the attractor, that demonstrate that the attractor generated by the fractional order system has a chaotic behavior. Finally, an electronic circuit is designed, considering the fractance device with the idea of approximate the integral operator of fractional order. The objectives considered to development this thesis are described below:

General objective

Propose a fractional order chaotic oscillator considering the unstable dissipative system and its electronic design.

Particular objectives

- To generate a fractional order unstable dissipative system considering the unstable dissipative system and analyze its stability.
- To design electronic oscillators based on fractional order unstable dissipative system.

Thesis contribution

In summary, the main contribution of this thesis is on the fractional order dynamical systems and on chaotic circuits. In particular, an approach to design an

electronic circuit which obeys to the same equations of the fractional order nonlinear system. In this endeavor, the contribution results of this thesis are listed in the following.

- A dynamical system, fractional order unstable dissipative system (FOUDS). This dynamical system is generated from the stability theorem related to fractional calculus.
- A study about the connection between the equilibrium points and eigenvalues of the system, and its reduction in effective dimension, which is the sum of all orders concerned to derivatives, in the proposed fractional order chaotic system.
- Integer order transfer functions to approximate fractional operators.
- An analog circuit design for the fractional order unstable dissipative system proposed.

Thesis organization

The rest of this thesis is organized as follows. In Chapter 1 a brief introduction about fractional calculus, some definitions related to stability of fractional order systems, and numerical algorithm to compute the solutions of fractional order systems are presented. Chapter 2 describes fundamentals concepts directly related to nonlinear systems. Chapter 3 introduces the fractional order unstable dissipative system, also gives a review of three well known integer order chaotic systems, and their fractional order representation. Besides, the chapter describes the computer-assisted verification of chaos in the fractional order unstable dissipative system by using the topological horseshoe theorem. In Chapter 4 describes the design and simulation of an analog electronic circuit that realizes the fractional order unstable dissipative system with low orders i.e., the section gives the basic blocks needed for the realization of an electronic circuit equivalent to a fractional order nonlinear system. Finally, in chapter 6 concludes the thesis and outlines some future research directions.

Chapter 1

Fractional Order Systems

In this chapter a brief introduction about fractional calculus is presented, a branch of mathematics that is, in a certain sense, as old as classical calculus as we know it today. Starting from fundamentals definitions of fractional calculus until a numerical method for solving fractional order differential equations, this chapter is a review of necessary concepts.

1.1 Fundamentals and definitions in fractional calculus

Fractional calculus is a generalization of differentiation and integration of functions to noninteger order, the continuous integro-differential operator ${}_aD_t^\alpha$, where a and t are the limits of the operation and $\alpha \in \mathbb{R}$. The operator is defined as

$${}_aD_t^\alpha = \begin{cases} \frac{d^\alpha}{dt^\alpha}, & \alpha > 0, \\ 1, & \alpha = 0, \\ \int_a^t (d\tau)^\alpha, & \alpha < 0. \end{cases}$$

Different definitions of fractional order integration and differentiation have emerged during the development of fractional order calculus theory. Some of the definitions are directly extended from the conventional order calculus. The most commonly used definitions are summarized as follows [5, 15, 16, 18, 27]:

A. Fractional order Cauchy integral formula

The formula is extended from integer order calculus

$$D^{\alpha}f(t)=\frac{\Gamma(\alpha+1)}{j2\pi}\int_{C}\frac{f(\tau)}{(\tau-t)^{\alpha+1}}d\tau, \tag{1.1}$$

where C is the closed path that encircles the poles of the function $f(t)$ [27]. The integrals and derivatives for cosine and sinusoidal functions can be expressed by

$$\frac{d^{k}}{dt^{k}}(\cos at)=a^{k}\cos\left(at+\frac{k\pi}{2}\right),\quad \frac{d^{k}}{dt^{k}}(\sin at)=a^{k}\sin\left(at+\frac{k\pi}{2}\right). \tag{1.2}$$

It can also be shown with Cauchy's formula that, if k is not an integer, the above formula is still valid.

B. Grünwald-Letnikov definition

The fractional order diferentiation and integral can be defined in a unified way, just as

$${}_{a}D_{t}^{\alpha}f(t)=\lim_{h\to 0}\frac{1}{h^{\alpha}}\sum_{j=0}^{\left[\frac{t-a}{h}\right]}(-1)^{j}\binom{\alpha}{j}f(t-jh), \tag{1.3}$$

where $\binom{\alpha}{j}$ are binomial coefficients, the subscripts to the left and right of D are the lower and upper bounds in the integral. The value of α can be positive or negative, i.e., corresponding to differentiation and integration, respectively and the α is noninteger

C. Riemann-Liouville definition

The fractional order integral is given by

$${}_{a}D_{t}^{-\alpha}f(t)=\frac{1}{\Gamma(\alpha)}\int_{a}^{t}\frac{f(\tau)}{(t-\tau)^{1-\alpha}}d\tau, \tag{1.4}$$

where $0<\alpha<1$, and a is the initial value. Let $a=0$, the notation of integral can be simplified to $D_{t}^{-\alpha}f(t)$. The Riemann-Liouville definition is a widely

used definition for fractional order differentiation and integral. Similarly, fractional order differentiation is defined as

$$ {}_aD_t^{\alpha} f(t) = \frac{d^n}{dt^n}\left({}_aD_t^{-(n-\alpha)} f(t)\right) = \frac{1}{\Gamma(n-\alpha)}\frac{d^n}{dt^n}\int_0^t \frac{f(\tau)}{(t-\tau)^{\alpha-n+1}}d\tau, \quad (1.5) $$

where $n = \lceil \alpha \rceil$.

D. Caputo definition

The Caputo fractional order differentiation can be written as

$$ {}_0D_t^{\alpha} f(t) = \frac{1}{\Gamma(n-\alpha)}\int_0^t \frac{f^n(\tau)}{(t-\tau)^{\alpha-n+1}}d\tau, \quad (1.6) $$

for $n = \lceil \alpha \rceil$. Similarly, by the Caputo definition, the integral is described by

$$ {}_0D_t^{-\alpha} f(t) = \frac{1}{\Gamma(\alpha)}\int_0^t \frac{f(\tau)}{(t-\alpha)^{1-\alpha}}, \quad \alpha > 0. \quad (1.7) $$

In the above definitions $\Gamma(\cdot)$ is the Gamma function,

$$ \Gamma(z) = \int_0^{\infty} t^{z-1}e^{-t}dt. \quad (1.8) $$

It can be show that for varieties of functions, Riemann-Liouville and Caputo are equivalent [16]

The main reason of considering the Caputo definition in this thesis is due to the fact of the initial conditions for the fractional order differential equations because are the same form as those integer order differential equations, and there are clear interpretations of the initial conditions for integer orders, moreover, it has the benefit of possessing a value of zero when it is applied to a constant. As well as ${}_0D_t^{\alpha} f(t)$ as $D^{\alpha} f(t)$ for simplicity in the notation in the following content.

The properties of fractional calculus are summarized as follows [16]:

A. If $f(t)$ is an analytical function of t, its fractional derivative $D^{\alpha} f(t)$ is an analytical function of t and α.

B. For $\alpha = n$, where n is an integer, the operation $D^{\alpha} f(t)$ gives the same result as classical differentiation of integer order n.

C. For $\alpha = 0$, the operator $D^{\alpha} f(t)$ is the identity operator

$$D^{0} f(t) = f(t).$$

D. Fractional differentiation and fractional integration are linear operations

$$D^{\alpha}(af(t) + bg(t)) = aD^{\alpha} f(t) + bD^{\alpha} g(t).$$

E. The additive index law (semigroup property)

$$D^{\alpha} D_t^{\beta} f(t) =_0 D^{\beta}{}_0 D^{\alpha} f(t) = D^{\alpha+\beta} f(t).$$

holds under some reasonable constraints on the function $f(t)$. The fractional order derivative commutes with integer order derivative

$$\frac{d^n}{dt^n}(D^r f(t)) = D^r \left(\frac{d^n f(t)}{dt^n} \right) =_a D^{r+n} f(t),$$

The relationship above says the operators $\frac{d^n}{dt^n}$ and $D^r f(t)$ commute [16].

1.2 Laplace transform of fractional order

The Laplace transform is one of the most useful tools for solving differential equations with initial conditions and solving engineering problems, in this way, recall some basic information with respect to Laplace transform.

The function $F(s)$ of the complex variable s is defined by

$$F(s) = L\{f(t); s\} = \int_0^{\infty} e^{-st} f(t) dt, \tag{1.9}$$

is known as the Laplace transform of the function $f(t)$. For the existence of integral (1.9) the function $f(t)$ there exist an exponential α, which means that there are positive constants M and T so that

$$e^{-\alpha t} |f(t)| \leq M, \text{ for all } t > T.$$

The $f(t)$ can be reestablished from the Laplace transform $F(s)$ with the help of the inverse Laplace transform

$$f(t) = L^{-1}\{F(s);t\} = \int_{c-j\infty}^{c+j\infty} e^{st}F(s)ds, \quad c = Re(s) > c_0, \tag{1.10}$$

where c_0 lies in the right half plane of the absolute convergence of the Laplace integral (1.10).

A property is the formula for the Laplace transform of the derivative of an integer order n of the function $f(t)$, expressed as $L\{\cdot\}$ is given by

$$L\{f^n(t);s\} = s^nF(s) - \sum_{k=0}^{n-1} s^{n-k-1}f^k(0) = s^nF(s) - \sum_{k=0}^{n-1} s^k f^{n-k-1}(0), \tag{1.11}$$

which can be obtained from the definition (1.11) by integrating by parts under the assumption that the corresponding integrals exist.

1.2.1 Laplace transform of fractional derivatives

The evaluation of the Laplace transform of the Riemann-Liouville fractional derivative, is written as follows

$$D^u f(t) = g^n(t), \tag{1.12}$$

$$g(t) = D^{-(n-u)}f(t)\frac{1}{\Gamma(k-u)}\int_0^t (t-\tau)^{n-u-1}f(\tau)d\tau, \quad n-1 \leq u < n. \tag{1.13}$$

Considering the formula for the Laplace transform of an integer order derivative (1.11) leads to

$$L\{D^u f(t)\} = s^n - G(s) - \sum_{k=0}^{n-1} s^k g^{n-k-1}(0). \tag{1.14}$$

The Laplace transform of the function $g(t)$ is evaluated by

$$L\{D^{-u}g(t)\} = L\{D^{-u}g(t)\} = s^{-u}G(s) \tag{1.15}$$

Hence, the following expression for the Laplace transform of the Riemann-Liouville fractional derivative of order $u > 0$

$$L\{D^u f(t)\} = s^u F(s) - \sum_{k=0}^{n-1} s^k (D^{u-k-1}f(t))_{t=0}, \quad n-1 \leq u < n. \tag{1.16}$$

The Laplace transform of the Caputo fractional derivative has the following form

$$L\{D^{\alpha}f(t)\} = s^{\alpha}F(s) - \sum_{k=0}^{n-1} s^{\alpha-k-1}f^{m}(0), \quad n-1 \leq \alpha < n. \tag{1.17}$$

The Laplace transform of a fractional order derivative for zero initial conditions can be expressed by [5, 15]

$$L\{D^{\alpha}f(t)\} = s^{\alpha}F(s). \tag{1.18}$$

Equation (1.18) is useful in order to calculate the inverse Laplace transform of elementary transfer functions, such as non integer order integrators e.g., $1/s^{\alpha}$. Indeed, replacing α with $-\alpha$ and considering the Dirac impulse as $f(t) = \delta(t)$, by means of the definition (1.6), it holds that

$$L\left\{\frac{t^{\alpha-1}}{\Gamma(\alpha)}\right\} = \frac{1}{s^{\alpha}}; \qquad L^{-1}\left\{\frac{1}{s^{\alpha}}\right\} = \left\{\frac{t^{\alpha-1}}{\Gamma(\alpha)}\right\}, \tag{1.19}$$

that is the impulse response of a non integer order integrator.

1.3 Fractional systems and state space representation

A general fractional order system can be described by a fractional differential equation of the form [15, 18]

$$\begin{aligned} a_n D^{\alpha_n}y(t) + a_{n-1}D^{\alpha_{n-1}}y(t) + \ldots + a_0 D^{\alpha_0}y(t) \\ = b_m D^{\beta_m}u(t) + b_{m-1}D^{\beta_{m-1}}u(t) + \ldots + b_0 D^{\beta_0}y(t), \end{aligned} \tag{1.20}$$

where $D^{\gamma} \equiv_0 D_t^{\gamma}$ denotes the Riemann-Liouville, The Grünwald-Letnikov or the Caputo's fractional derivative [1, 5, 16, 18]. The corresponding transfer function considering incommesurate (non-identical fractional order) real orders has the following form [15]

$$G(s) = \frac{b_m s^{\beta_m} + \ldots + b_1 s^{\beta_1} + b_0 s^{\beta_0}}{a_n s^{\alpha_n} + \ldots + a_1 s^{\alpha_1} + a_0 s^{\alpha_0}} = \frac{Q(s^{\beta_k})}{P(s^{\alpha_k})} \tag{1.21}$$

where α_k with $(k = 0,\ldots,n)$, β_k with $(k = 0,\ldots,m)$ are arbitrary real or rational numbers that can be organized as $\alpha_n > \alpha_{n-1} > \cdots > \alpha_0$, and $\beta_n > \beta_{n-1} > \cdots > \beta_0$ and a_k with $(k = 0,\ldots,n)$, b_k with $(k = 0,\ldots,m)$ are constant.

The incommensurate order system (1.21) can also be expressed in incommensurate form by the multivalued transfer function [15]

$$H(s) = \frac{b_m s^{\beta/v} + \ldots + b_1 s^{1/v} + b_0}{a_n s^{\alpha/v} + \ldots + a_1 s^{1/v} + a_0}, \quad (v > 1). \tag{1.22}$$

Observe that every fractional order system can be expressed in the form (1.22) and the domain of $H(s)$ is a Riemann surface with v Riemann sheets [18].

In commensurate order systems, a general expression can be introduced, consider that, $\alpha_k = \alpha k$, $\beta_k = \alpha k$ with $(0 < \alpha < 1), \forall k \in Z$, finally the transfer function has the following form:

$$G(s) = K_0 \frac{\sum_{k=0}^{M} b_k (s^\alpha)^k}{\sum_{k=0}^{N} a_k (s^\alpha)^k} = K_0 \frac{Q(s^\alpha)}{P(s^\alpha)}, \tag{1.23}$$

where $N > M$, the function $G(s)$ becomes a proper rational function in the complex variable s^α which can expanded in partial fractions of the following form:

$$G(s) = K_0 \left[\sum_{i=1}^{N} \frac{A_i}{s^\alpha + \lambda_i} \right], \tag{1.24}$$

with $\lambda_i (i = 1, 2, \ldots, N)$ are the roots of the pseudo-polynomial $P(s^\alpha)$.

The analytical solution of the system (1.24) can be expressed by

$$y(t) = L^{-1} \left\{ K_0 \left[\sum_{i=1}^{N} \frac{A_i}{s^\alpha + \lambda_i} \right] \right\} = K_0 \sum_{i=1}^{N} A_i t^\alpha E_{\mu,\xi}(-\lambda_i t^\alpha), \tag{1.25}$$

where $E_{\mu,\xi}$ is the Mittag-Leffler function is defined by [16]

$$E_{\mu,\xi}(z) = \sum_{i=0}^{\infty} \frac{z^i}{\Gamma(\mu i + \xi)} \quad (\mu > 0, \xi > 0), \tag{1.26}$$

where for instance $E_{1,1}(z) = e^z$.

Consider a fractional order derivative equation system as follows

$$a_n D^{\alpha_n} y(t) + a_{n-1} D^{\alpha_{n-1}} y(t) + \ldots + a_0 D^{\alpha_0} y(t) = u(t), \tag{1.27}$$

by Laplace transform, is possible obtain a fractional transfer function

$$G(s) = \frac{Y(s)}{U(s)} = \frac{1}{a_n s^{\alpha_n} + \ldots + a_1 s^{\alpha_1} + a_0 s^{\alpha_0}}, \tag{1.28}$$

The fractional order linear time invariant (LTI) system can also be represented by the following state space model [18]

$$\begin{aligned} D_t^{\mathbf{q}} x(t) &= \mathbf{A}x(t) + \mathbf{B}u(t) \\ y(t) &= \mathbf{C}x(t) \end{aligned} \tag{1.29}$$

where $x \in \mathbb{R}^n$, $u \in \mathbb{R}^r$ and $y \in \mathbb{R}^p$ are the state, input and output vectors of the system, $\mathbf{A} \in \mathbb{R}^{n\times n}$, $\mathbf{B} \in \mathbb{R}^{n\times r}$, $\mathbf{C} \in \mathbb{R}^{p\times n}$, and $\mathbf{q} = [q_1, q_2, \ldots, q_n]^T$ are the fractional orders. If the orders $q_1, q_2, \ldots, q_n \equiv \alpha$, the system (1.29) is called a commensurate order system, otherwise it is an incommensurate order system.

State transition matrix is

$$\begin{aligned} \mathbf{x}(t) &= \left[\mathbf{I} + \frac{\mathbf{A}\mathbf{x}(0)}{\Gamma(1+\alpha)}t^{\alpha} + \frac{\mathbf{A}^2\mathbf{x}(0)}{\Gamma(1+2\alpha)}t^{2\alpha} + \ldots \frac{\mathbf{A}^k\mathbf{x}(0)}{\Gamma(1+k\alpha)}t^{k\alpha} + \ldots\right] \\ &= \left(\sum_{k=0}^{\infty} \frac{\mathbf{A}^k t^{k\alpha}}{\Gamma(1+k\alpha)}\right) x(0) = \mathbf{\Phi}(t)\mathbf{x}(0). \end{aligned} \tag{1.30}$$

A fractional order system described by n-term fractional differential equation (1.27) can be written into state space representation in the form [15, 28]

$$\begin{aligned} \begin{pmatrix} D^{q_1}x_1(t) \\ D^{q_2}x_2(t) \\ \vdots \\ D^{q_n}x_n(t) \end{pmatrix} &= \begin{pmatrix} 0 & 1 & \ldots & 0 \\ 0 & 0 & 1\ldots & 0 \\ \vdots & \vdots & \ddots & \vdots \\ -a_0/a_n & -a_1/a_n & \ldots & a_{n-1}/a_n \end{pmatrix} \begin{pmatrix} x_1(t) \\ x_2(t) \\ \vdots \\ x_n(t) \end{pmatrix} + \begin{pmatrix} 0 \\ 0 \\ \vdots \\ 1/a_n \end{pmatrix} u(t), \\ y(t) &= \begin{pmatrix} 1 & 0 & \ldots & 0 & 0 \end{pmatrix} \begin{pmatrix} x_1(t) \\ x_2(t) \\ \vdots \\ x_n(t) \end{pmatrix}, \end{aligned} \tag{1.31}$$

where $\alpha_0 = 0, q_1 = \alpha_1, q_2 = \alpha_{n-1} - \alpha_{n-2}, \ldots q_n = \alpha_n - \alpha_{n-1}$, with initial conditions

$$\begin{aligned} x_1(0) &= x_0^1 = y_0, \quad x_2(0) = x_0^2 = 0, \ldots \\ x_i(0) &= x_0^i = \begin{cases} y_0^k, & \text{if } i = 2k+1, \\ 0 & \text{if } i = 2k, \end{cases} \qquad i \le n. \end{aligned} \tag{1.32}$$

The $n-$term fractional order differential equation (1.27) is equivalent to the system of equations (1.31) with the initial conditions (1.32) in the Caputo sense [7, 29].

1.4 Stability of fractional order systems

Stability as an important property of dynamical systems, its usually refers to the qualitative behavior of motions relative to an invariant set. It is well known from the theory of stability that a linear time invariant (LTI) system is stable if the roots of the characteristic polynomial are negative or have negative real parts if they are complex conjugate. It means that they are located on the left half of the imaginary axis of complex $s-$plane. The domain can be viewed as a Riemann surface with finite number of Riemann sheets v, where the origin is a branch point and the branch cut is assumed an $\mathbb{R}^-$. The branch cut is assumed at $\mathbb{R}^-$ and the first Riemann sheet is denoted by Ω and defined by

$$\Omega = \{re^{j\phi} | r > 0, -\pi < \phi < \pi\}. \tag{1.33}$$

In the fractional order LTI case, the stability is different from the integer case [27]. An interesting point is that a stable fractional system may have roots in right half of the complex $w-$plane Fig. 1.1. Since the main sheet of the Riemann surface is defined $-\pi < \arg(s) < \pi$, by considering the mapping $w = s^\alpha$, the domain of w is defined by $-\alpha\pi < \arg(w) < \alpha\pi$ and the w plane region corresponding to the right half plane of this sheet is described by $-\alpha\pi/2 < \arg(w) < \alpha\pi/2$. It has been shown that system (1.29) is stable if the following condition is satisfied [30, 31].

Theorem 1.4.1. *[30, 31] A commensurate order SISO system described by the fractional transfer function (1.21) is stable if only if following condition is satisfied*

$$|\arg(\lambda_i)| > \frac{\alpha\pi}{2}, \quad \textit{for all i,} \tag{1.34}$$

with λ_i the $i-$root of pseudo-polynomial $P(\cdot)$.

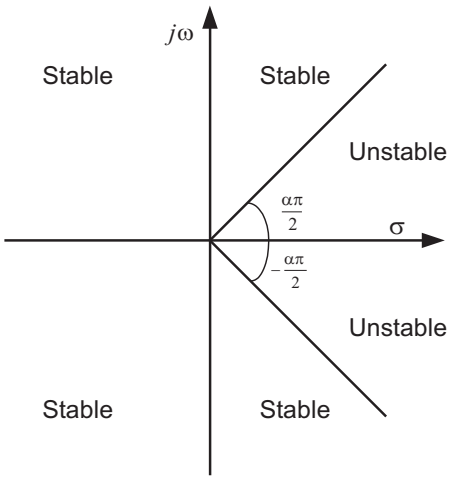

Figure 1.1: Stability region of LTI fractional order systems with order $0 < \alpha < 1$.

Generally, consider the following commensurate fractional order system in the form

$$D^{\boldsymbol{\alpha}}\mathbf{x} = \mathbf{f}(x), \tag{1.35}$$

here $\boldsymbol{\alpha} = [\alpha_1, \alpha_2, \ldots, \alpha_n]^T$ for $0 < \alpha_i < 1$, $(i = 1, 2, \ldots, n)$ and $\mathbf{x} \in \mathbb{R}^n$. The equilibrium points of system (1.35) are calculated via solving the following equation

$$\mathbf{f}(\mathbf{x}) = 0, \tag{1.36}$$

where $x^* = (x_1^*, x_2^*, \ldots, x_n^*)$ is an equilibrium point of the system (1.35). The equilibrium points are asymptotically stable if all the eigenvalues λ_i, $(i = 1, 2, \ldots, n)$ of the Jacobian matrix $J = \partial\mathbf{f}/\partial\mathbf{x}$, satisfy the following condition

$$|\arg(eig(J))| = |\arg(\lambda_i)| > \frac{\alpha\pi}{2}, \quad i = 1, 2, \ldots, n. \tag{1.37}$$

Figure 1.1 shows the stable and unstable regions of the complex plane for such a case.

1.5 Numerical method for solving fractional differential equations.

Similar to integer-order systems, the solution of the fractional systems is computed using a numerical integration algorithm. The Adams-Bashforth-Moulton (ABM) method, a predictor-corrector scheme, reported in [32] is used herein to obtain the time evolution of fractional order differential equations. The algorithm is a generalization of the classical Adams-Bashforth-Moulton integrator that is well known for the numerical solution of first-order problems [33,34]. I select the ABM as numerical solver because of it is based on the Caputo derivatives which allows us to specify both homogeneous and inhomogeneous initial conditions contrary to Riemann-Liouville-based methods.

Consider the following fractional order differential equation:

$$\begin{aligned} D^{\alpha}y(t) &= f(t,y(t)), \quad 0 \le t \le T; \\ y^{(k)}(0) &= y_0^{(k)}, \qquad k = 0,1,\ldots,n-1. \end{aligned} \tag{1.38}$$

The solution of (1.38) is given by an integral equation of Volterra type as

$$y(t) = \sum_{k=0}^{\lceil\alpha\rceil-1} y_0^k \frac{t^k}{k!} + \frac{1}{\Gamma(\alpha)} \int_0^t (t-z)^{\alpha-1} f(z,y(z))dz. \tag{1.39}$$

How it is showed in [6], there is a unique solution of (1.38) on some interval $[0,T]$, thence we are interested in a numerical solution on the uniform grid $\{t_n = nh | n = 0,1,\ldots,N\}$ with some integer N and stepsize $h = T/N$, then (1.39) can be replaced by a discrete form to get the corrector as follows

$$\begin{aligned} y_h(t_{n+1}) &= \sum_{k=0}^{\lceil\alpha\rceil-1} y_0^k \frac{t^k}{k!} + \frac{h^{\alpha}}{\Gamma(\alpha+2)} f\left(t_{n+1}, y_h^p(t_{n+1})\right) \\ &\quad + \frac{h^{\alpha}}{\Gamma(\alpha+2)} \sum_{j=0}^{n} a_{j,n+1} f\left(t_j, y_h(t_j)\right), \end{aligned} \tag{1.40}$$

where

$$a_{j,n+1} = \begin{cases} n^{\alpha+1} - (n-\alpha)(n+1)^{\alpha}, \quad j = 0, \\ (n-j+2)^{\alpha+1} + (n-j)^{\alpha+1} \\ \quad -2(n-j+1)^{\alpha+1}, \quad 1 \leq j \leq n, \\ 1, \quad j = n+1, \end{cases} \tag{1.41}$$

Moreover, the predictor has the following structure

$$y_h^p(t_{n+1}) = \sum_{k=0}^{\lceil \alpha \rceil - 1} y_0^k \frac{t^k}{k!} + \frac{1}{\Gamma(\alpha)} \sum_{j=0}^{n} b_{j,n+1} f(t_j, y_h(t_j)), \tag{1.42}$$

with $b_{j,n+1}$ defined by

$$b_{j,n+1} = \frac{h^{\alpha}}{\alpha}((n+1-j)^{\alpha} - (n-j^{\alpha})). \tag{1.43}$$

The error of this approximation is given by

$$\max_{j=0,1,\ldots N} |y(t_j) - y_h(t_j))| = \mathcal{O}(h^P), \tag{1.44}$$

where $P = \min(2, 1+\alpha)$. It important to mention that in this thesis, a fractional order dynamical systems are considered, so the algorithm (1.40) and (1.42) is employed to obtain a numerical solution for each one fractional differential equation. Finally, in Appendix B the pseudocode of the algorithm is presented.

In this chapter it has been presented a historical review and fundamental definitions about fractional calculus that give the idea that this fractional calculus is as rigorous as its counterpart classical integer order differentiation and integration, moreover, the state space representation of dynamical systems, and the algorithm for the numerical solution of differential equations of fractional order, taking into account initial conditions.

Chapter 2

Fractional Order Dynamical Systems

The fractional order nonlinear dynamics systems are used to describe a vast variety of science and engineering phenomena. This chapter describes the fundamental concepts and tools that are directly related to nonlinear dynamics that are briefly review in this thesis.

2.1 Elementary dynamical systems theory

Most continuous-time fractional order nonlinear dynamical systems studied in this thesis are described by either a fractional order differential equation. Consider the following fractional order nonlinear system in the from

$$D^{\boldsymbol{\alpha}} x = \mathbf{f}(\mathbf{x}, t; \mathbf{p}), \qquad t \in [t_0, \infty) \tag{2.1}$$

where $\boldsymbol{\alpha} = [\alpha_1, \alpha_2, \ldots, \alpha_n]$, for $0 < \alpha_i < 1$, $(i = 1, 2, \ldots, n)$ for $x = x(t)$ is the state vector of the system belonging to region $\Omega \subset \mathbb{R}^n$, $\mathbf{p}$ is a vector of system parameters, that may be allowed to vary within a interval $\mathbb{I}^n \subset \mathbb{R}^m$, often $m \leq n$, and $f(\cdot, \cdot)$ is a continuous nonlinear function.

The system (2.1) has a unique solution corresponding to any given initial condition, $x(t_0) = x_0 \in \Omega$ at the initial time $t_0 = 0$ [6,35]. The entire space $\mathbb{R}^n \times [0, \infty)$, to which the system states belong, is called the state space.

The fractional order dynamical system (2.1) is said to be autonomous, if the variable, t, does not appear independently in the system function $f(\cdot)$; in this case

$$D^{\boldsymbol{\alpha}} x = \mathbf{f}(\mathbf{x}; \mathbf{p}), \tag{2.2}$$

otherwise, (2.1) it is said to be nonautonomous. Obviously, in this thesis the state vector $x = x(t)$ is always a function of time.

A dynamical system is deterministic, if there is a unique consequence to every change of the system parameters or initial states, and it is stochastic, if there is more than one possible consequence for a change in its parameters or initial states according to some probability distribution [35].

2.2 Nonlinear dynamical systems

Consider a general two one-dimensional state variable system

$$\begin{aligned} D^{\alpha}x_1 &= f_1(x_1, x_2), \\ D^{\alpha}x_2 &= f_2(x_1, x_2), \end{aligned} \tag{2.3}$$

where $0 < \alpha < 1$, with initial conditions $(x_1(0), x_2(0))$ and two smooth nonlinear functions, $f_1(\cdot,\cdot)$ and $f_2(\cdot,\cdot)$. Here (f_1, f_2) describes the vector field of the system.

The trajectory traveled by the solution of the system (2.3), starting from the initial state $(x_1(0), x_2(0))$, which is a solution trajectory, or an orbit of the system. A solution of (2.3), with initial state $(x_1(0), x_2(0))$ is usually denoted by $\varphi(x_1(0), x_2(0))$. The family of φ_t, $t \in [0, \infty)$, satisfies $\varphi_{t_1+t_2} = \varphi_{t_1} \circ \varphi_{t_1}$, where $\varphi_{t_0}(x_1(0), x_2(0)) = (x_1(0), x_2(0))$. Since, for autonomous systems, two different solution trajectories never cross each other in the $x_1 - x_2$ plane, any solution $\varphi_t(x_1, x_2)$ of an autonomous system, considered as a family of trajectories with different initial conditions, is called flow in the $x_1 - x_2$ plane. All the possible solution trajectories of an autonomous system, plotted in the $x_1 - x_2$ plane corresponding to different initial conditions, constitute the phase portrait of the system solutions.

Equilibria of the system (2.3), if exist, are the solutions that simultaneously satisfy the homogeneous equation (1.36), the equilibria is usually denoted by (x_1, x_2). An equilibria is stable if all the nearby trajectories of the system, starting from any initial states, approach it; it is said to be unstable, if the nearby trajectories move

away from it. Equilibria can be classified, according to their stabilities, as stable or unstable node, node, focus, saddle point or center.

Let λ_1, λ_2 be the eigenvalues of the Jacobian matrix $J = \partial f/\partial x$, all evaluated at the equilibrium (x_1, x_2). As is well known,

$$\lambda_{1,2} = \frac{1}{2}\left[trace(J) \pm \sqrt{D}\right], \tag{2.4}$$

where $D = \left[trace(J)^2 - 4\det(J)\right]$. The different equilibria and their stabilities, determined by these two eigenvalues are summarized in Fig 2.1 [35, 36]

If the two eigenvalues of J satisfy $\mathbb{R}\{\lambda_{1,2}\} \neq 0$, then the equilibrium x^*, about which the linearization is taken, is said to be hyperbolic.

Consider the homogeneous linear system

$$D^\alpha x(t) = Ax(t), \quad x(t) \in \mathbb{R}^n, \tag{2.5}$$

where A is a $n \times n$ constant matrix, $x(0) = x_0$, and α is restricted in $(0, 1)$.

Definition 2.2.1. *[37] If all eigenvalues $\lambda(\mathbf{A})$ of $\mathbf{A}$ satisfy: $|\lambda(\mathbf{A})| \neq 0$ and $|\arg(\lambda(\mathbf{A}))| \neq \alpha\pi/2$, then the origin O of the linear system is called a hyperbolic equilibrium point.*

Definition 2.2.2. *[37] The autonomous system* (2.5) *is said to be: (1) stable if $\forall x_0$, there exists a $\epsilon > 0$ such that $||x(t)|| < \epsilon$ for $t \geq 0$; (2) asymptotically stable if $\lim_{t\to\infty} ||x(t)|| = 0$.*

The autonomous nonlinear differential system in the sense of Caputo is given as follows:

$$D^\alpha \mathbf{x}(t) = \mathbf{f}(\mathbf{x}(t)) \tag{2.6}$$

where $\mathbf{x}(t) \in \mathbb{R}^n$, $x(0) = x_0$, $\mathbf{f}(\mathbf{x})$ is continuous.

Definition 2.2.3. *The point e is an equilibrium point of system* (2.6)*, if and only if $f(e) = 0$.*

Definition 2.2.4. *[37] Suppose that e is an equilibrium point of system* (2.6)*, and that all the eigenvalues $\lambda(Df(e))$ of the linearized matrix $Df(e)$ at the equilibrium point e satisfy:$|\lambda(Df(e))| \neq 0$ and $|\arg(\lambda(Df(e)))| \neq \alpha\pi/2$, then we call e a hyperbolic equilibrium point.*

Definition 2.2.5. 1) *The equilibrium point e of* (2.6) *is said to be: (1) locally stable if* $\forall \epsilon > 0$, *there exists a* $\delta > 0$ *such that* $||x(t) - e|| < \epsilon$ *holds for* $\forall x_0 \in \{z : ||z - e|| < \delta\}$ *and* $\forall t > 0$; *(2) locally asymptotically stable if the equilibrium point is locally stable and* $\lim_{t \to +\infty} x(t) = e$.

2) *Denote* $x(t), \tilde{x}(t)$ *as the solution of the system* (2.6) *with initial values* $x_0, \tilde{x}_0$ *respectively. The solution* $x(t)$ *is said to be: (1) locally stable if* $\forall \epsilon > 0$, *there exists a* $\delta > 0$ *such that* $||x(t) - \tilde{x}(t)|| < \epsilon$ *holds for* $||x_0 - \tilde{x}_0|| < \delta$ *and* $\forall t \geq 0$*; (2) locally asymptotically stable if the solution is locally stable and* $\lim_{t \to +\infty}(x(t) - \tilde{x}(t)) = 0$.

Suppose $f(x_1), g(x_2)$ are continuos vector fields defined on $U, V \subset \mathbb{R}^n$, and they generate a flow $\varphi_{t,f} : U \to U$, $\varphi_{t,g} : V \to V$.

Definition 2.2.6. *If there is a homeomorphism* $h : U \to V$, *satisfying:* $h \circ \phi_{t,f}(x) = \varphi_{t,g} \circ h(x), x \in \delta(x_0, r) \subset U, x_0 \in U$ *then* $f(x_1)$ *and* $g(x_2)$ *are locally topologically equivalent. If the above relation holds in the whole space* U*, then they are globally topologically equivalent.*

The linearization theorem of fractional differential equation with Caputo derivative. Without loss of generality, let e be the origin.

Theorem 2.2.1. *[37] If the origin* O *is a hyperbolic equilibrium point of* (2.6)*, then vector field* $\mathbf{f}(\mathbf{x})$ *is topologically equivalent with its linearization vector field* $Df(0)x$ *in the neighborhood* $\delta(0)$ *of the origin* O.

The above theorem can be regarded as the fractional version of the Hartman theorem [37], this theorem guarantees that for hyperbolic case, one can study the linearized system intend of original nonlinear system, with regard to the local dynamical behavior of the system within a neighborhood of the equilibrium x^*. In other words, there are some homeomorphic maps that transform the trajectories of the nonlinear system into trajectories of its linearized system in a neighborhood of the equilibrium.

2.2.1 Attractors and limit sets

In the theory of dynamical system, steady states of the system solutions refer to the asymptotic behaviors of the solution as $t \to \infty$. Certainly, only those bounded steady states are meaningful. A solution trajectory between its initial state and steady state is called the transient state. Yet, there is generally no clear-cut line between transient and steady states, unless a transition point is specified [35].

For a given dynamical system, a point x_2 in the space state is said to be an $\omega-$limit point of an orbit $x(t)$ of the system, if for each open neighborhood U_{x_2} of x_2, the trajectory of $x_1(t)$ enters U_{x_2} at a large enough but fine value of t. Moreover, the trajectory $x_1(t)$ will repeatedly enter any given neighborhood of x_2, no matter how small it is as $t \to \infty$. The set of all $\omega-$limit points of $x_1(t)$ denoted by L_{x_1} is called the $\omega-$limit set of $x_1(t)$. An $\omega-$limit set L_{x_1} is attracting if there is an open neighborhood U_L of L_{x_1}, such that, if the trajectory of a system state enters U_L at some initial instant $t_1 \geq t_0$ then this trajectory will approach L_{x_1} arbitrary closely, as $t \to \infty$. The basin of attraction of an attracting point is the union of all such open neighborhoods. An $\omega-$limit set is repelling if the system trajectory always moves away from it [35, 36].

An attractor is defined to be the union of all those points in a attracting set that is invariant under the system operators or iterations of the underlying map. In other words, an attractor is an $\omega-$limit set, L_{x_1}, satisfying the property that all orbits near L_{x_1} have L_{x_1} as their $\omega-$limit sets.

2.2.2 Poincaré map

Consider both n and p integers the $n-$dimensional nonlinear autonomous system (2.2) and assume that this system has a t_p-periodic limit cycle Γ. Let x^* be a point on the list cycle and Σ be an $(n-1)^p-$dimensional hyperplane transversal to Γ at x^*. The transversality of Σ to Γ at x^* means that Σ and the tangent line of Γ at x^* span the entire $n-$dimensional space [35].

Since Γ is a periodic orbit, the trajectory starting from the point x^* will return to x^* in one period of time, t_p. Any trajectory starting from a point called x in

a small neighborhood U_{x^*} of x^* on Σ, will return and cross Σ at a point denoted $P(x)$, in the vicinity V_{x^*} of x^*. Therefore, a map $P : U_{x^*} \to V_{x^*}$, can be defined by Σ along with the solution flow of the autonomous system. This map is called the Poincaré map associated with the system and the cross-section Σ.

2.2.3 Homoclinic and heteroclinic trajectories

Let x^* be a hyperbolic equilibrium of a $P : \mathbb{R}^n \to \mathbb{R}^n$ of unstable, center or saddle type. Let $\varphi_t(x)$ be a solution trajectory that pass through x^* and L_{x^*} be the limit set of $\varphi_t(x)$. The stable manifold of L_{x^*} denoted by M_s is the set points x such that $\varphi_t(x)$ approaches L_{x^*} as $t \to \infty$. The unstable manifold of x^* denoted M_u is the set of points x such that $\varphi_t(x)$approaches L_{x^*} as $t \to -\infty$ [38].

Suppose that $\Sigma_s(x^*)$ and $\Sigma_u(x^*)$ are cross-section of the stable and unstable manifolds of $\varphi_t(x)$, and they intersect at x^*. This intersection includes one constant trajectory: $\varphi_t(x) = x^*$. A non constant trajectory lies in the intersection $\Sigma_s(x^*) \cap \Sigma_u(x^*)$ is called a homoclinic trajectory. Consider two equilibria $x_1^* \neq x_2^*$ of unstable, center or saddle type, a trajectory that lies in $\Sigma_s(x_1^*) \cap \Sigma_u(x_2^*)$ or $\Sigma_u(x_1^*) \cap \Sigma_s(x_2^*)$ is called a heteroclitic trajectory. A heteroclitic trajectory approaches one equilibrium point as $t \to \infty$ and approaches a different equilibrium point as $t \to -\infty$ [35, 38].

Let x^* be a hyperbolic unstable fixed point of a diffeomorphism $P : \mathbb{R}^n \to \mathbb{R}^n$. Suppose $\Sigma_s(x^*)$ and $\Sigma_u(x^*)$ interesect at a point $x_0 \neq x^*$. Let $\{x_k\}_{k=-\infty}^{\infty}$ be the orbit through x_0. Where the sequence $\{x_k\}$ is a homoclinic orbit and each x_k is called a homoclinic point. Since x_0 lies in both the stable and unstable manifolds, so does the homoclinic orbit $\{x_k\}$. It follows that if the stable and unstable manifolds intersect at a point other than x^*, then the intersect at an infinite number of points [38].

This structure is called a homoclinic structure. In this the two manifolds usually do not intersect transversally, so the structure is unstable in the sense that the connection can be destroyed by small perturbations. Still, if they intersect transversally, the transversal homoclinic point will imply infinitely other homo-

clinic points, what eventually leads to extremely complicated stretching and folding of the two manifolds. Such stretching and folding manifolds are key to chaos. Now, is important consider that a transversal homoclinic point implies the existence of a Smale horseshoe map, embedding in the diffeomorphism P [38–40]. This result is proved in the Smale-Birkhoff homoclinic theorem.

Theorem 2.2.2. *[35, 38] Let $P : \mathbb{R}^n \to \mathbb{R}^n$ be a diffeomorphism with a hyperbolic equilibrium x^*. If the cross-sections of the unstable and stable manifolds, $\Sigma_u(x^*)$ and $\Sigma_s(x^*)$, intersect transversally at a point other than x^*, then P has a horseshoe map embedded within it.*

The three one-dimensional variable systems, that have an equilibrium with a real eigenvalue λ and two complex conjugate eigenvalues $a \pm jb$. Consider the case when $\lambda > 0$ and $a < 0$ gives a $Shilikov - type$ of homoclinic trajectory with the following result [35, 38]

Theorem 2.2.3. *[35, 38] Let φ_t be the solution flow of a three dimensional autonomous system that has a Shilnikov-type homoclinic trajectory, γ. If $|a| < |\lambda|$, then φ_t can be perturbed to $\tilde{\varphi}_t$ extremely slightly, such that $\tilde{\varphi}_t$ has a homoclinic trajectory $\tilde{\gamma}$, near γ, of the same type, and the Poincaré map, defined by a cross-section transversal to $\tilde{\gamma}$, has a countable set of Smale horseshoe.*

2.3 Smale Horseshoe

A common analysis to verify the chaotic behavior of a dynamical system is carried out by computing its Lyapunov exponents due to they are a good tool to characterize the high sensitivity to the initial conditions. Nevertheless, when dealing with chaotic systems, sometimes it is difficult to get Lyapunov exponents with high computation accuracy because it may also depends on the length of time computed as well as the step-size used to numerical integration algorithms [41, 42]. Therefore, the largest Lyapunov exponent seems insufficient to validate absolutely the chaotic behavior of fractional order systems, since it may simply

produce an unbounded system trajectory, and yet if the trajectories are bounded then the system is likely chaotic, in addition especially when the computed value of this exponent is close to zero, and the numerical error may cause a bias.

On the other hand, the topological horseshoe theory, which is based on the notion of symbolic dynamics [38, 39, 41–44], provides a proof to estimate topological entropy, verifies existence of chaos, and reveals invariant sets of chaotic attractors in chaotic systems. The topological horseshoe depends on the geometry of continuous maps on some subsets of interest in state space based on the second return Poincaré map, for continuous-time systems the topological horseshoe theorem cannot be directly applied [43, 44]. Therefore, one needs to find an appropriate Poincaré section to obtain a Poincaré map.

The basic procedure is to propose an appropriate Poincaré section and define a second return Poincaré map, which implies that the entropy of the attractors of fractional order nonlinear dynamical system is not less than $\log 2$, giving a compelling signature of chaos.

2.3.1 Aspects of symbolic dynamics.

Let $S_m = \{0, 1, \ldots, m-1\}$ and $\sum_m$ be the collection of all bi-infinite sequences with their elements $s \in \sum_m$:

$$s = \{\ldots, s_{-n}, \ldots, s_{-1}, s_0, s_1, \ldots, s_n, \ldots\}, \quad s_i \in S_m, \forall i.$$

If we consider another sequence $\bar{s} \in \sum_m$, with

$$\bar{s} = \{\ldots, \bar{s}_{-n}, \ldots, \bar{s}_{-1}, \bar{s}_0, \bar{s}_1, \ldots, \bar{s}_n, \ldots\}, \quad \bar{s}_i \in S_m, \forall i.$$

Then the distance between s and $\bar{s}$ is defined as

$$d(s, \bar{s}) = \sum_{-\infty}^{\infty} \frac{1}{2^{|i|}} \frac{|s_i - \bar{s}_i|}{1 + |s_i - \bar{s}_i|}. \tag{2.7}$$

2.3.2 Metric space and the *m*-shift.

With the distance defined in (2.7), $\sum_m$, is a metric space and with the following three properties with which a set is called a Cantor set [39].

Theorem 2.3.1. *[39, 41] The metric space $\sum_m$ is compact, totally disconnected and perfect.*

Now define a map of $\sum_m$ into itself, denoted by γ, as follows:

$$\gamma(s_i) = s_{i+1}, \quad \forall i. \tag{2.8}$$

The map γ is called an *m*-shift map, which has the following properties.

Theorem 2.3.2. *[39] (a)* $\gamma(\sum_m) = \sum_m$, and γ is continuous; *(b)* The shift map γ as a dynamical system defined on $\sum_m$ has:
(i) a countable infinity of periodic orbits consisting of orbits of all periods;
(ii) an un-countable infinity of non-periodic orbits;
(iii) a dense orbit.

In this manner the dynamics generated by the shift map γ displays sensitive dependence on initial conditions on a closed invariant set and transitivity, therefore it is chaotic. (See [38–44] for proofs of the theorems.)

Let X be a metric space, D be a compact subset of X, and $f : D \to X$ be a map satisfying the assumption that there exist m mutually disjoint subsets $D_1, \ldots, D_{m-1}$ and D_m of D, so that the restriction of f to each D_i, $f|Di$, is continuous, for all $i = 1, \ldots, m-1$.

Definition 2.3.1. *[28] Let ξ be a compact subset of D, such that for every $1 \leq i \leq m$, $\xi_i = \xi \bigcap D_i$ is nonempty and compact. Then ξ is called a connection with respect to $D_1, \ldots, D_{m-1}$ and D_m. Let F be a family of connections with respect to $D_1, \ldots, D_{m-1}$ and D_m, satisfying the property:*

$$\xi \in F \Rightarrow f(\xi_i) \in F.$$

Then F is said to be an f-connected family with respect to $D_1, \ldots, D_{m-1}$ and D_m.

Definition 2.3.2. *[39] If there is a continuous and onto map*

$$h : K \to \sum_m$$

such that $h \circ f = \gamma \circ h$, then f is said to be a semi-conjugate to γ.

Theorem 2.3.3. *[39,41] If there is an f-connection family with respect to $D_1, D_2, \ldots, D_m$, then there is a compact invariant set $K \subset D$, such that $f|K$ is semi-conjugate to an m-shift map.*

Theorem 2.3.4. *[41] For two dynamical systems (X, f) and (Y, g), if (X, f) is semi-conjugate to (Y, g), then the topology entropy of f is not less than that of g.*

The topological entropy is a nonnegative real number. Then the system is chaotic if its topological entropy is not zero. Furthermore, if g is an m-shift map, then $ent(f) \geq ent(g) = \log m$, that is, f is chaotic when $m > 1$.

2.4 Chaos

There is no universally agreed definition of chaos in the literature. Among a few definitions given in mathematical terms are two slightly different but well accepted ones, one given by Li and Yorke where formally begin the use of the name chaos in the modern scientific and engineering literature [35], while the second is perhaps better known. The second definition given by Devaney states that a map, $M : S \to S$, where S is generally a compact and invariant set under M in $\mathbb{R}^n$, is said to be chaotic if [35, 45]:

- M is **transitive** on S, in the sense that for any pair of nonempty open set U and V in S, there is an integer $k > 0$, such that $M^k(U) \cap V$ is nonempty;
- the periodic points of M are **dense** in S;
- M has a **sensitive dependence on initial conditions**, i.e., there is a real number $\delta > 0$ depending only on M and S, such that in every nonempty open subset of S there are a pair of points whose eventually iterates under M are separated by a distance of at least δ.

Some different characteristics about chaos have been analyzed and observed, for instance, the extreme sensitive to initial conditions; a hallmark of chaos, in the

sense that two sets of similar initial conditions can give rise to two different asymptotic states of the system trajectory. Positive Lyapunov exponents that measure the rate of divergence of nearby trajectories; in specific the positive Lyapunov exponent is the time average logarithm growth rate of the maximal distance between to nearby orbits, and is perhaps the most convenient one to verify in engineering applications. Kolmogorov-Sinai entropy another hallmark, used the idea related to the static entropy, which is a measure of the amount information that is needed to determined the state of the systems to define a measure for the intensity of a set of systems states, which gives the mean loss information on the state of a system when it evolves with the time. This measure can also be used to characterize strange attractors and chaos. The simple zero of the Melnikov theory function provides a measure of the distance between a stable and unstable manifold. The Melnikov theory gives that chaos is possible if these manifolds intersect, which corresponds to that the Melnikov function has a simple zero, and can be used to characterize chaos focuses on the saddle points of Poincaré maps of continuous flows in the phase space. Among others, that are consider the hallmark of chaos.

In this chapter, it has been presented an elementary dynamical systems theory. This theory gave the essential background to verify the chaotic behavior in a nonlinear dynamical system, for instance, the Poincaré map, the Smale's horseshoe, such theory provided an analysis to verify the chaotic behavior. moreover the classification of two-dimensional equilibria.

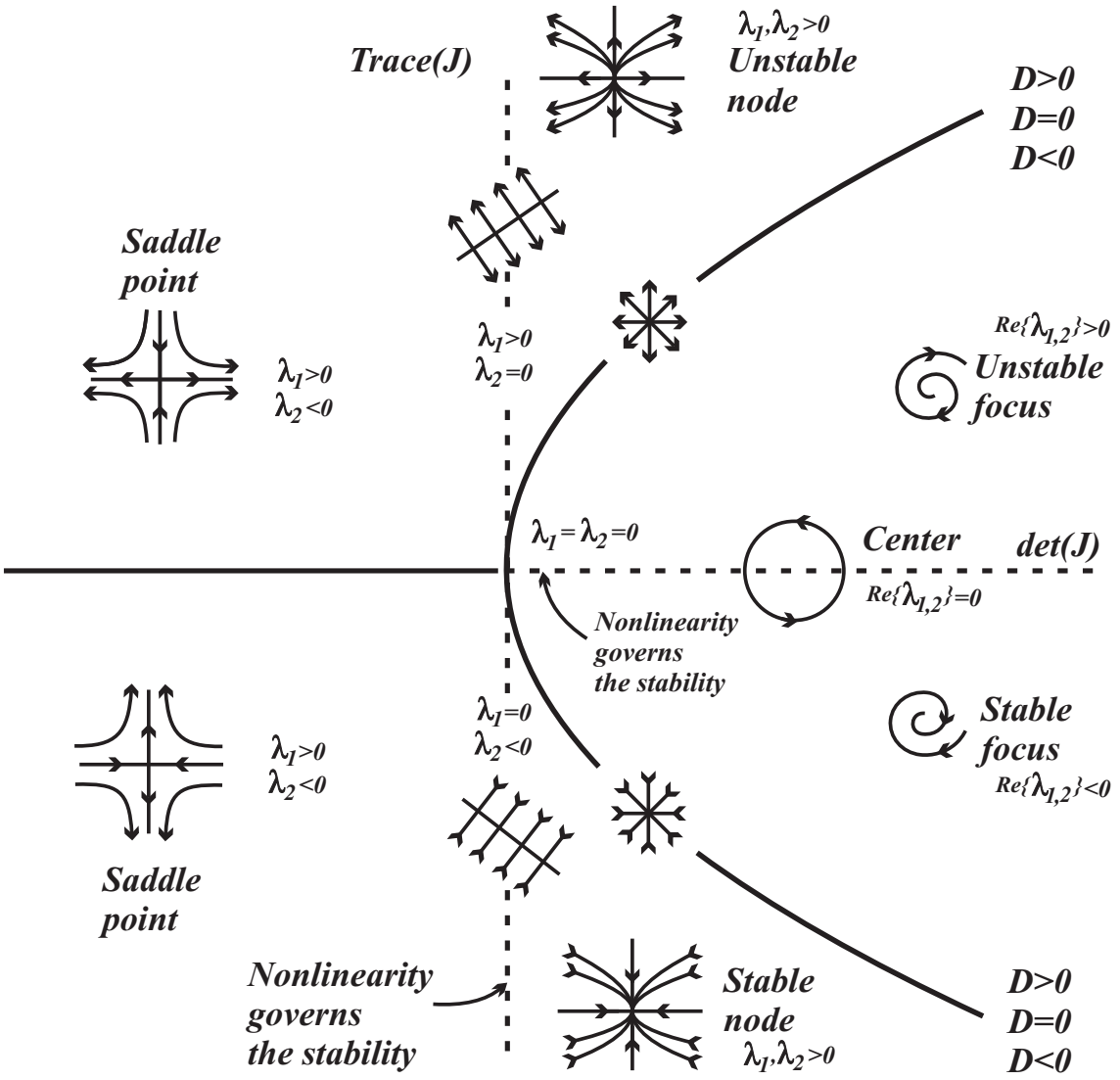

Figure 2.1: Classification of two dimensional equilibria: stabilities are determined by their eigenvalues.

Chapter 3

Dynamics of Fractional Order UDS systems

In this section a fractional order unstable dissipative system with only two equilibrium points is presented. Based on the integer version of an unstable dissipative system and using the same system's parameters.

3.1 Fractional order unstable dissipative system

A dynamical system is called unstable dissipative system (UDS) if the system dynamical has a saddle-focus equilibrium which is responsible for stable and unstable manifolds and the sum of its eigenvalues is negative, and a dynamical systems is called FOUDS when the Unstable Dissipative Systems is of Fractional Order. As much as FOUDS and UDS are built with a switching law to obtain a strange attractor. The strange attractor appears as a result of the unification of several unstable one-spiral trajectories. Each of these trajectories lies around a saddle hyperbolic equilibrium point [46].

Consider the fractional order affine linear system given by

$$D^{\alpha}\mathbf{x} = \mathbf{A}\mathbf{x} + \mathbf{B} \tag{3.1}$$

where $\mathbf{x} = [x_1, \ldots, x_n]^T \in R^n$ is the state vector, $\mathbf{B} = [B_1, \ldots, B_n]^T \in R^n$ stands for a real vector, $\mathbf{A} = [a_{ij}] \in R^{n \times n}$ denotes a linear operator, $\alpha = [\alpha_1, \ldots, \alpha_n]$ taking

into account $0 < \alpha_i < 1$. Considering that $\mathbf{A}$ is not singular then the equilibrium point is located at $x^* = -\mathbf{A}^{-1}\mathbf{B}$. The dynamics of the system is given by matrix $\mathbf{A}$ due to define a vector field $\mathbf{Ax}$. So, suppose that the matrix $\mathbf{A}$ has j negative eigenvalues $\lambda_1, \ldots, \lambda_j$ and $n-j$ positive eigenvalues $\lambda_{j+1}, \ldots, \lambda_n$. Let $\{v_1, \ldots, v_n\}$ be the corresponding set of eigenvectors. Then the stable and unstable subspaces of the affine linear system (3.1), E^s and E^u, are the linear subspaces spanned by $\{v_1, \ldots, v_j\}$ and $\{v_{j+1}, \ldots, v_n\}$ respectively

$$E^s = Span\{v_1, \ldots, v_j\},$$
$$E^u = Span\{v_{j+1}, \ldots, v_n\},$$

According to the above information and considering real and complex eigenvalues, it is possible to define a FOUDS as follows:

Definition 3.1.1. *The fractional order system* (3.1) *is said to be FOUDS if* $|\arg(\lambda_i)| > \alpha\pi/2$ *and* $\sum_{i=1}^{n} \lambda_i < 0$*, with* $i = 1, \ldots, n$*, and at least one* λ_i *is a positive real eigenvalue or two* λ_i *are complex eigenvalues with positive real part* $Re\{\lambda_i\} > 0$*. None of them is pure imaginary eigenvalue.*

Definition 3.1.2. *Let the system (3.1) be a FOUDS with ordered real and complex eigenvalues set* $\Lambda = \{\lambda_1, \ldots, \lambda_n\}$ *and* $Re\{\lambda_1\} \leq \ldots \leq Re\{\lambda_j\} < 0 < Re\{\lambda_{j+1}\} \leq \ldots \leq Re\{\lambda_n\}$*. Then, the system has a stable manifold* $E^s \subset R^n$ *and another unstable* $E^s \subset R^n$ *with* $1 \leq j \leq n$ *and*

- *All the initial condition* $x_0 \in E^u$ *leads to an unstable trajectory that goes to infinity.*
- *All the initial condition* $x_0 \in E^s$ *leads to a stable trajectory that settle down at* $x*$ *and the system does not generate oscillations.*
- *The basin of attraction* $\mathbf{B}$ *is* $E^s \subset \mathbb{R}^n$

The switching system based on the affine linear system (3.1) as follows

$$D^{\boldsymbol{\alpha}}\mathbf{x} = \mathbf{Ax} + \mathbf{B}(x) \tag{3.2}$$

$$\mathbf{B}(x) = \begin{cases} B_1, & \text{if} \quad x \in V_1 \\ \vdots & \vdots \\ B_k, & \text{if} \quad x \in V_k. \end{cases} \tag{3.3}$$

Where $\mathbb{R}^n = \cup_{i=1}^{k} V_i$ and $\cap_{i=1}^{k} V_i = \emptyset$, and $\alpha = [\alpha_1, \ldots, \alpha_k]$ taking into account $0 < \alpha_i < 1$. Therefore the equilibria of the system (3.2) is defined as $x_i^* = -\mathbf{A}^{-1} B_i$ with $i = 1, \ldots, k$. The main idea is related to define vectors B_i, these vectors can generate a class of dynamical systems in $\mathbb{R}^n$ with a behavior that converge into a chaotic attractor, that is mean, the flow $\phi_t(x(0))$ of the system (3.3) tends in an attractor called $\boldsymbol{\Xi}$ by defining at least two vectors B_1 and B_2. Each domain, $V_i \subset \mathbb{R}^n$ contains the equilibrium $x_i^*, = -\mathbf{A}^{-1} B_i$.

Remark According to the above discussion is possible define a multi-scroll chaotic attractor based on FOUDS.

Definition 3.1.3. *[47] A fractional order system given by (3.2) with equilibria x_i^*, with $i = 1, \ldots, k$ and $k > 2$. Then the fractional order system (3.2) generates a multi-scroll chaotic attractor $\boldsymbol{\Xi} \subset \mathbb{R}^n$ if each x_i^* have oscillations around and the flow $\phi_t(x_0)$*
.

A consequence of the previous discussion, it is possible to define two types of FOUDS in $\mathbb{R}^3$, according to their corresponding equilibria.

Definition 3.1.4. *[47] Consider the fractional order system (3.1) in $\mathbb{R}^3$ with eigenvalues λ_i, $i = 1, 2, 3$ such that $\sum_{i=1}^{3} \lambda_i < 0$. and $|\arg(\lambda_i)| > \alpha\pi/2$. Then, the system is said to be an FOUDS of **type I** if one of its eigenvalues is negative real and the other two are complex conjugate with positive real part; and it is to be of **type II** if one of its eigenvalues is positive real and the other two are complex conjugate with negative real part.*

In this thesis, only the commutation between FOUDS of **type I** is considered, i.e., fractional order commensurate systems that consider three one dimensional variable.

The following double scroll chaotic system by switching linear systems; based on a fractional order jerk equation written in the form

$$\begin{aligned} D^{\alpha}x &= y, \\ D^{\alpha}y &= z, \\ D^{\alpha}z &= -ax - by - cz + B, \end{aligned} \tag{3.4}$$

where $\boldsymbol{\alpha}= [\alpha, \alpha, \alpha]$ with all the elements inside the vector are equals moreover $\alpha \in (0,1), a, b, c, B \in \mathbb{R}$, could be any arbitrary scalars that satisfy the Definition 3.1.4, thus the dynamics of the switched system of equation (3.3), where the matrix A and the vector B can be represented as follows:

$$\mathbf{A} = \begin{pmatrix} 0 & 1 & 0 \\ 0 & 0 & 1 \\ -a & -b & -c \end{pmatrix}; \quad \mathbf{B} = \begin{pmatrix} 0 \\ 0 \\ B \end{pmatrix}. \tag{3.5}$$

The characteristic polynomial of matrix A given by (3.5) gets the following

$$\lambda^3 + c\lambda^2 + b\lambda + a. \tag{3.6}$$

For sake of simplicity the coefficient a is varying in $\mathbb{R}$ while that the other two coefficients are fixed in $b = 1, c = 1$. So the coefficient should be guarantee that the system will be an UDS I or UDS II, for instance the UDS I is given when for $a > 1$, and the UDS II for $a < 0$. Likewise, the coefficient is setting in $a = 1.5$ to assure the UDS I. In addition, the eigenvalues with these values are $\lambda_1 = -1.2041, \lambda_{2,3} = 0.1020 \pm 1.1115i$ satisfying the Definition 3.1.4 for UDS I. The parameter B is the switched control law defined as follows [46]:

$$B = \begin{cases} B, & \text{if} \quad x \geq 0.35, \\ 0, & \text{if} \quad x < 0.35. \end{cases} \tag{3.7}$$

The equilibrium points and its eigenvalues of the system in (3.2) using the matrix $\mathbf{A}$ and vector $\mathbf{B}$ defined in (3.5) and the switching control law (3.7) are given in Table 3.1. The system has only two equilibrium points O and E_1 which are saddle points of instability index two; therefore, there is a double-scroll attractor given by the fractional order system .

Table 3.1: Equilibrium points and corresponding eigenvalues.

Equilibrium point	Eigenvalues
$O(0,0,0)$	$-1.2041, 0.1020 \pm 1.1115i$
$E_1(0.66,0,0)$	$-1.2041, 0.1020 \pm 1.1115i$

3.1.1 Fractional order to generate chaotic behavior on FOUDS

In order to obtain chaotic behavior from FOUDS, the stability general theorem 1.4.1 given in section 1.4 must be satisfied. As a result, the system (3.4) displays regular and stable behavior if it satisfies (1.34)

$$\alpha < \frac{2}{\pi} \min_i |\arg(\lambda_i)| \approx 0.9417 \tag{3.8}$$

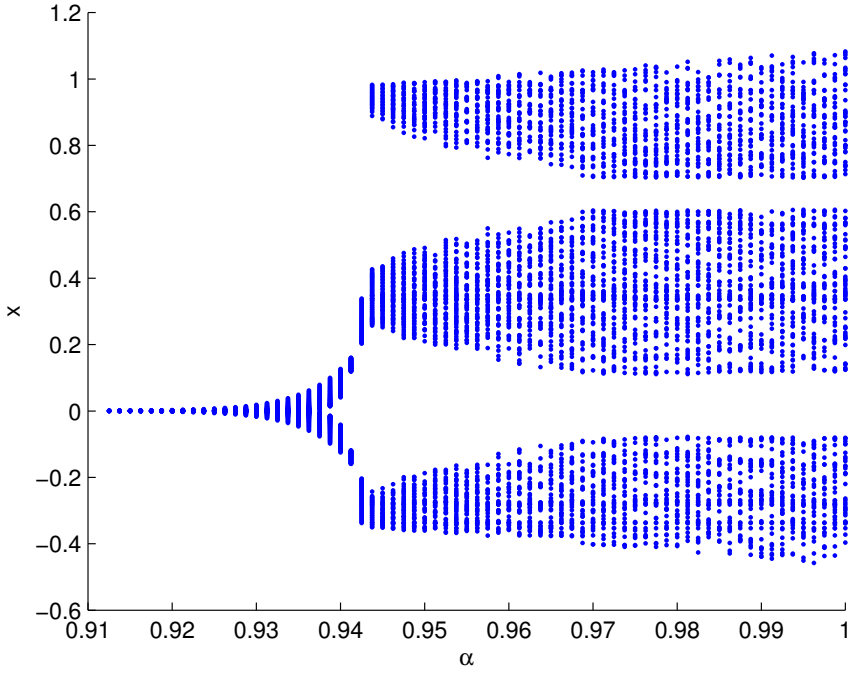

Figure 3.1: Bifurcation diagram of FOUDS system for the commensurate fractional order $\alpha \in [0.91, 1]$.

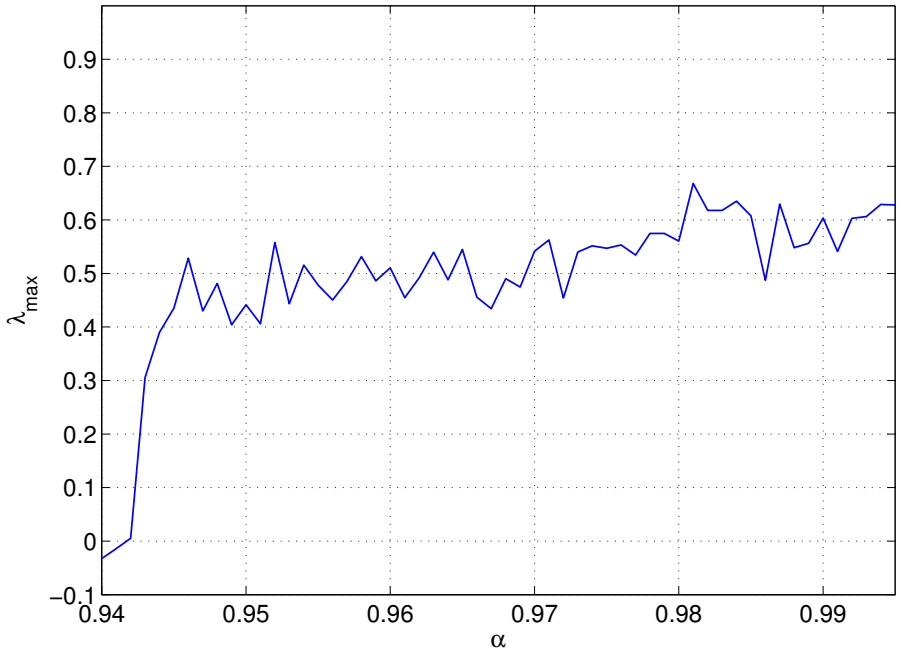

Figure 3.2: Largest Lyapunov exponent of the proposed fractional system in (3.4) for cases in Table 3.2 respectively. The horizontal axis represents fractional order α with dimensionless, the vertical axis represents the magnitude of $\lambda_{\max}$.

Accordingly, the system does not show chaotic behavior for $\alpha < 0.9417$. This result is supported by bifurcation diagram and largest Lyapunov exponent (LLE). The Fig. 3.1 shows the bifurcation diagram of the system (3.4) against the commensurate fractional order $\alpha \in [0.91, 1]$. The bifurcation diagram shows the Poincaré section $y(t) = 0$ projected onto the x axes for varying values of α between 0.91 and 1. The Figure 3.2 shows the largest Lyapunov exponent $\lambda_{\max}$ for the attractors of FOUDS in Fig. 3.3 as a function of the fractional order α. The largest Lyapunov exponent is computed from the numerical time series of the state-variable x using TISEAN package software due to it has been appointed as a proved tool to investigate the presence of chaos in several numerical and experimental systems [48]. As a result, FOUDS shows chaotic behavior because of it has an attractor with a positive Lyapunov exponent at least. We observe this behavior in

the approximate range of $\alpha \in [0.95, 0.99]$ by considering the system's parameters $a = 1.5, b = 1, c = 1, B = 1.5$. Furthermore, as demonstrated in Fig. 3.3 a) where the projection of the attractor onto the xy-plane for $\alpha = 0.94$ is displayed, and shows that the system does not display chaotic behavior. Hence, in order to show that FOUDS can generate fractional chaotic behavior we consider $\alpha \geq 0.95$. Fig. 3.3 b) shows the projection of the chaotic attractor onto the xy-plane for $\alpha = 0.95$. Figs. 3.3 c) to f) show the projections of the attractors onto the xy-plane for $\alpha = 0.96, 0.97, 0.98, 0.99$, respectively. This set of chaotic attractors has the same number of equilibria as scrolls. By usign the same parameters as integer-order case, we observe that FOUDS generates fractional chaos behavior with an effective minimum dimension as low as 2.85. Table 3.2 summarizes the results.

Table 3.2: Parameters for which FOUDS generates chaotic behavior.

Order α	System's parameters	Behavior	$\lambda_{\max}$	Phase portrait
0.94	$a = 1.5,\ b = 1,\ c = 1,$ $B = 1$	Fixed point		Fig. 3.3 a)
0.95	$a = 1.5,\ b = 1,\ c = 1,$ $B = 1$	Chaos	0.44	Fig. 3.3 b)
0.96	$a = 1.5,\ b = 1,\ c = 1,$ $B = 1$	Chaos	0.51	Fig. 3.3 c)
0.97	$a = 1.5,\ b = 1,\ c = 1,$ $B = 1$	Chaos	0.54	Fig. 3.3 d)
0.98	$a = 1.5,\ b = 1,\ c = 1,$ $B = 1$	Chaos	0.56	Fig. 3.3 e)
0.99	$a = 1.5,\ b = 1,\ c = 1,$ $B = 1$	Chaos	0.6	Fig. 3.3 f)

Table 3.2 shows that the magnitude of the largest Lyapunov exponent depends on the fractional order α.

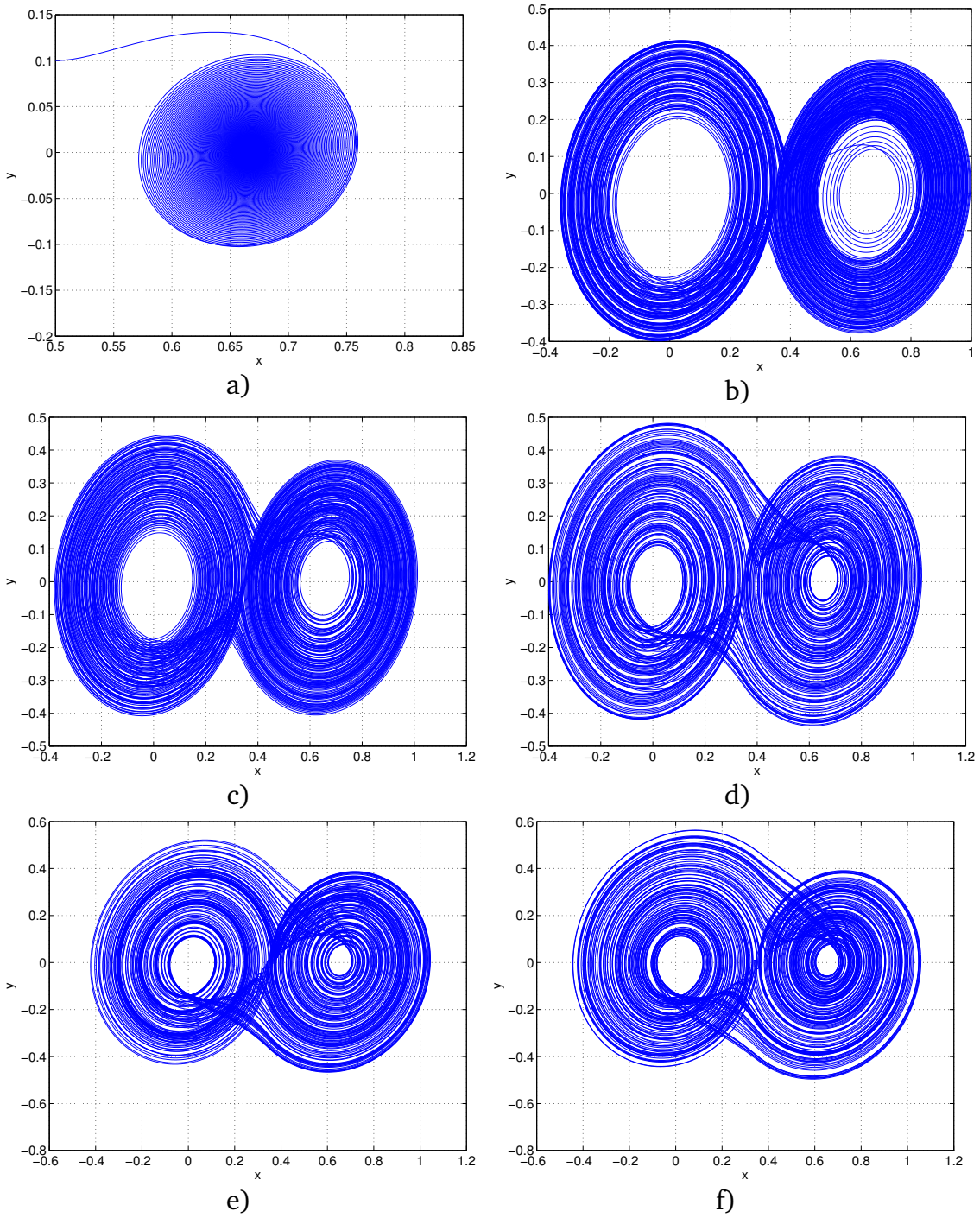

Figure 3.3: Projections of the attractors onto the xy-plane for parameters given in Table 3.2.

3.2 Analysis of FOUDS with different values in the parameters

As second case, other values for system's parameters a, b, c, and function switching law are proposed in order to find chaos behavior with lower fractional orders. By means of considering the strange attractor that appears as a result of the combination of several unstable one-spiral trajectories around a saddle hyperbolic stationary point, the corresponding eigenvalues are scaled in a proper form to preserve the chaotic regime and the asymptotic stability from (section 1.4). Notice that the equilibrium points (Table 3.1) together with commutation plane are identical as integer-order case. It means a and B must be chosen in a convenient way to preserve the relation $B/a = 0.66$, where the relation is related to equilibrium point.

Chaotic attractors of FOUDS are observed for two different sets of parameters, given in Table 3.3, as shown in Figs. 3.4 d) to f). Compared to previous case chaos can be obtained with lower dimensions of 2.49, 2.46, and 2.4 respectively. Similarly, the largest Lyapunov exponent of these attractors is plotted versus α in Fig. 3.4 b). Again, the fractional system in (3.4) presents chaotic behavior in the approximate interval of $\alpha \in [0.815, 0.84]$ with $a = 4.75, b = 0.9, c = 0.9, B = 3.16$. In addition, regular oscillations are found when the system's parameters do not fulfill the stability condition, as displayed in Figs. 3.4 a) to c).

3.3 Topological analysis of FOUDS

The Smale horseshoe or the topological horseshoe theory, provides a method to study the chaotic characteristic in the nonlinear dynamical systems. The existence of horseshoe in nonlinear dynamical systems is the most remarkable characteristic of chaos.

A Smale horseshoe map is a sequence of basic topological operations consist of stretching which gives sensitivity to initial conditions, and folding which gives the

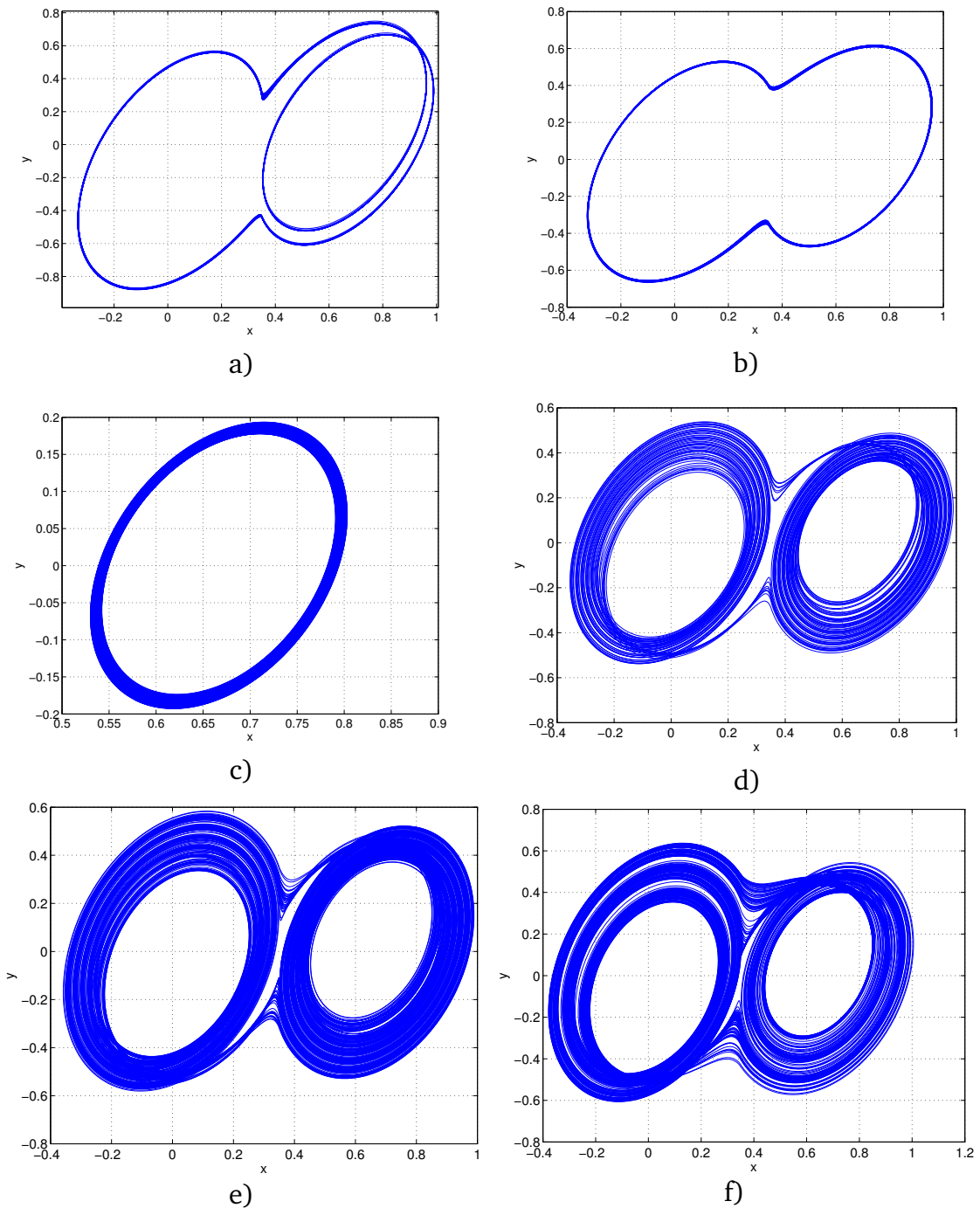

Figure 3.4: Projections of the attractors onto the xy-plane for parameters given in Table 3.3.

Table 3.3: Parameters for which FOUDS generates regular oscillations and chaotic behavior with low orders.

Order α	System's parameters	Behavior	$\lambda_{\max}$	Phase portrait
0.7	$a=7.5$, $b=0.2$, $c=0.2$, $B=5$	Limit cycle		Fig. 3.4 a)
0.74	$a=4.5$, $b=0.3$, $c=0.3$, $B=3$	Limit cycle		Fig. 3.4 b)
0.77	$a=3$, $b=0.5$, $c=0.5$, $B=3$	Limit cycle		Fig. 3.4 c)
0.8	$a=3.75$, $b=0.7$, $c=0.7$, $B=2.5$	Chaos	0.4	Fig. 3.4 d)
0.82	$a=4.75$, $b=0.9$, $c=0.9$, $B=3.16$	Chaos	0.53	Fig. 3.4 e)
0.83	$a=4.75, b=0.9$, $c=0.9$, $B=3.16$	Chaos	0.66	Fig. 3.4 f)

attraction. Since trajectories in phase space cannot cross, the repeated stretching and folding operations result in an object of great topological complexity [49]. The theory concerns on a set Q (usually diffeomorphic to a rectangle) in a two-dimensional manifold M and a diffeomorphism $f : Q \to M$. By considering only hypotheses on the first iterate of f on Q, Smale concludes that there is a compact invariant set Q_I in Q which is homeomorphic to a shift on 2 symbols [50].

This section proves the existence of a topological horseshoe in a double-scroll chaotic attractor, where first select a suitable Poincaré section, and then prove that the corresponding Poincaré map is semi-conjugate to 2-shift map. This implies that the chaotic attractor studied has large topological entropy.

3.4 Horseshoe in the fractional order unstable dissipative system

In this subsection, prove the existence of the horseshoe in the fractional order system in (3.4) based on the review of the section 2.3.

First, the plane $\Omega = \{(x, y, z) \in R^3 : x = 0\}$ which is shown in Fig. 3.6 is proposed considering the FOUDS in (3.4) with $a = 4.75, b = 0.9, c = 0.9, B = 3.16$. On this

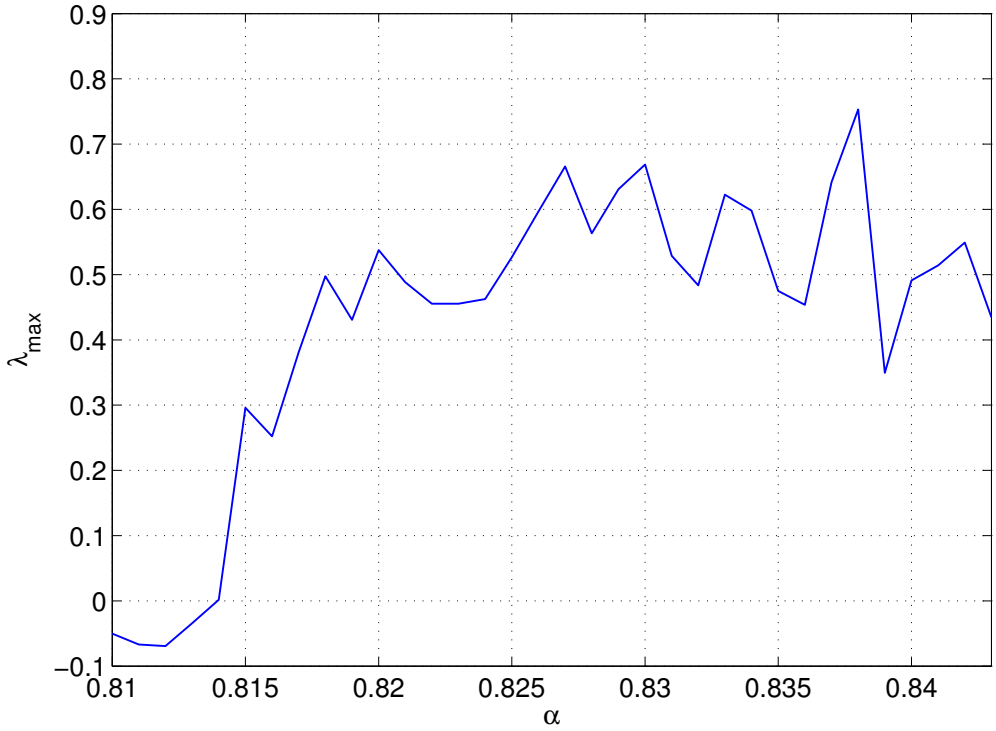

Figure 3.5: Largest Lyapunov exponent of the proposed fractional system in (3.4) for cases in Table 3.3 respectively. The horizontal axis represents fractional order α with dimensionless, the vertical axis represents the magnitude of $\lambda_{\max}$.

plane, we choose a Poincaré section with its four vertices being

$$A(0, 0.45, 0.48),\ B(0, 0.53, 0.538),$$

$$C(0, 0.54, 0.498),\ D(0, 0.46, 0.44).$$

The Poincaré map

$$P : |ABCD| \to \Omega,$$

is defined as follows. For each point $x \in |ABCD|,\ P(x)$ is chosen to be the second return intersection point with Ω under the flow of the system (3.4) with initial condition x. Under this Poincaré map P, $P(x)$ is very thin hook-like strip which is

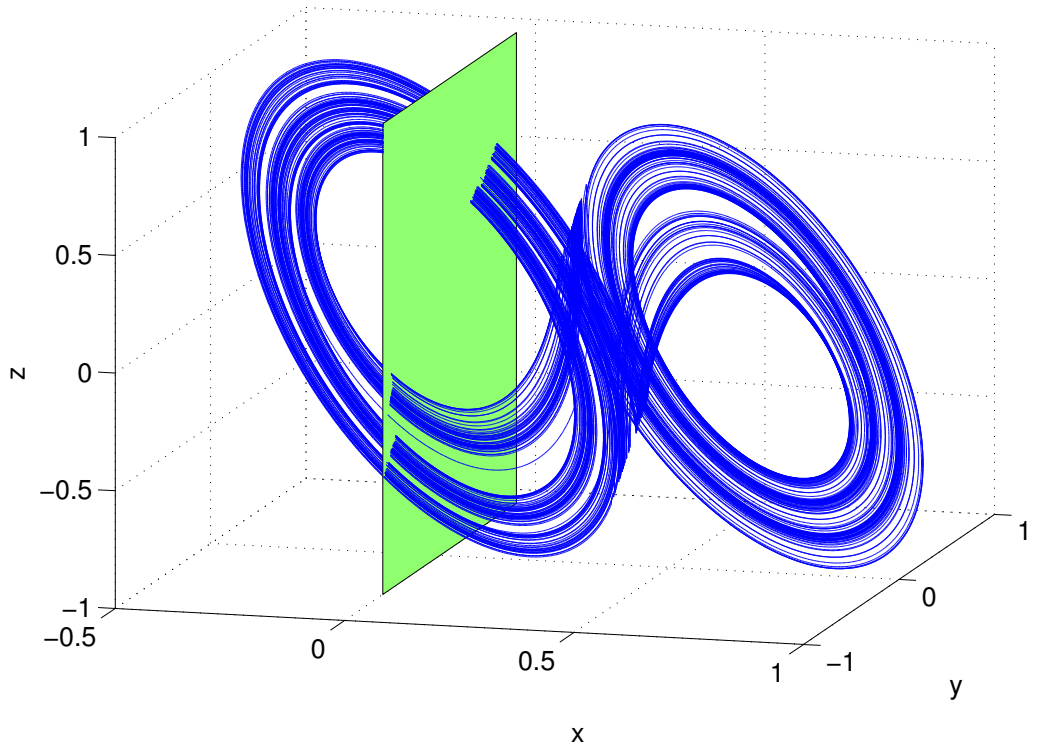

Figure 3.6: Chaotic attractor of the FOUDS with parameters $a = 4.75, b = 0.9, c = 0.9, B = 3.16$.

wholly across $|ABCD|$ as shown in Fig. 3.7, where

$$A' = P(A),\ B' = P(B),\ C' = P(C),\ D' = P(D),$$

are the images of points, respectively.

Theorem 3.4.1. *The Poincaré map P corresponding to the Poincaré section $|ABCD|$ has the property that there is a closed invariant set $\Lambda \subset |ABCD|$for which $P|\Lambda$ is semi conjugate to the 2-shift map, Hence,$ent(P) \geq \log 2 > 0$. This implies that attractor generated by the proposed FOUDS in (3.4) with $a = 4.75, b = 0.9, c = 0.9, B = 3.16$, has a positive topological entropy.*

Proof. In order to prove the assertion, one must find two mutually disjointed subsets of $|ABCD|$, such that a P-connected family with respect to them exists.

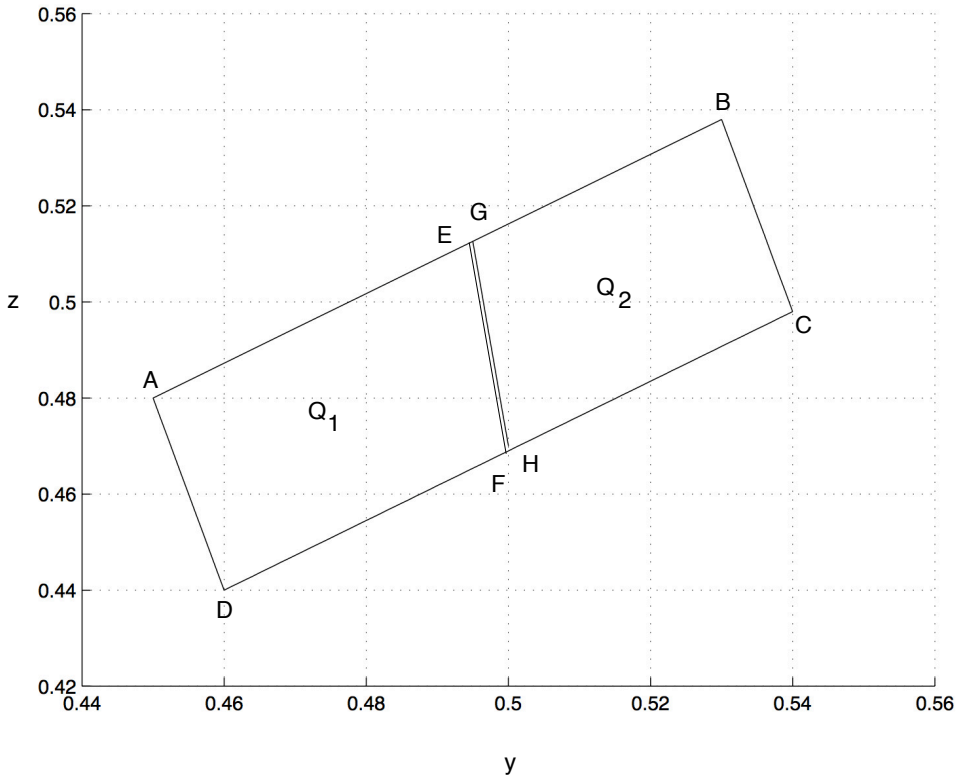

Figure 3.7: Two mutually disjoint subsets $|AEFD|$ and $|GBCH|$ of the quadrangle $|ABCD|$.

The subsets are denoted by Q_1 and Q_2 as shown in Fig. 3.7, the first subset Q_1 with the quadrangle $|ADEF|$. Under the first return Poincaré map P, the subset Q_1 is mapped to $|A'D'E'F'|$ with AD mapped to $A'D'$ and EF mapped to $E'F'$. We can make the conclusion that the image $P(Q_1)$ lies wholly across the quadrangle $|ABCD|$ with respect to AD and BC as shown in the Fig. 3.8.

The second subset Q_2, namely quadrangle $|GBCH|$, with GH and BC being its bottom and top edges, respectively. Like Q_1 the subset Q_2 is mapped to $|G'B'C'H'|$ under the Poincaré map P with GH mapped to $G'H'$ and BC mapped to $B'C'$. Thus, the image $P(Q_2)$ lies wholly across the quadrangle $|ABCD|$ with respect to

AD and BC as shown in the Fig. 3.9.

Evidently, the subsets Q_1 and Q_2 are mutually disjointed. Therefore, it follows that for every connection of $|ABCD|$ respect Q_1 and Q_2, for instance, Q_5, the images $P(Q_5 \cap Q_1)$ and $P(Q_5 \cap Q_2)$ also lie wholly across the quadrangle $|ABCD|$. Thus the images of $P(Q_5 \cap Q_1)$ and $P(Q_5 \cap Q_2)$ are still connections respect to Q_1 and Q_2. According to Definition 2.3.1 and Theorem 2.3.3, there is a P-connected family, so that the Poincaré map P is semi conjugate to the 2-shift map. Based on Theorem 2.3.4, it is concluded that the entropy of P is not less than $\log 2$, which implies that the attractors in Figs. 3.4 e) and f) have a positive entropy. The proof is completed.

Similarly, we apply the same proof to demonstrate the topological horseshoe when $a = 3.75, b = 0.7, c = 0.7, B = 2.5$, are selected as system's parameters of FOUDS in (3.4), the corresponding attractor is shown in Fig. 3.4 d). In this plane, i.e., $x = 0$, we set a Poincaré section with its four vertexes being

$$\hat{A}(0, 0.4, 0.45), \hat{B}(0, 0.45, 0.475),$$

$$\hat{C}(0, 0.5, 0.45), \hat{D}(0, 0.45, 0.4).$$

The Poincaré map

$$\hat{P} : |\hat{A}\hat{B}\hat{C}\hat{D}| \to \hat{\Omega},$$

is defined as follows. For each point $x \in |\hat{A}\hat{B}\hat{C}\hat{D}|, \hat{P}(x)$ is chosen to be the first return intersection point with $\hat{\Omega}$ under the flow of the system (3.4) with initial condition x. Under this Poincaré map $\hat{P}$, $\hat{P}(x)$ is a very thin hook-like strip which is wholly across $|\hat{A}\hat{B}\hat{C}\hat{D}|$ as shown in Fig. 3.10, where

$$\hat{A}' = \hat{P}(\hat{A}),\ \hat{B}' = \hat{P}(\hat{B}),\ \hat{C}' = \hat{P}(\hat{C}),\ \hat{D}' = \hat{P}(\hat{D}),$$

are the images of points, respectively.

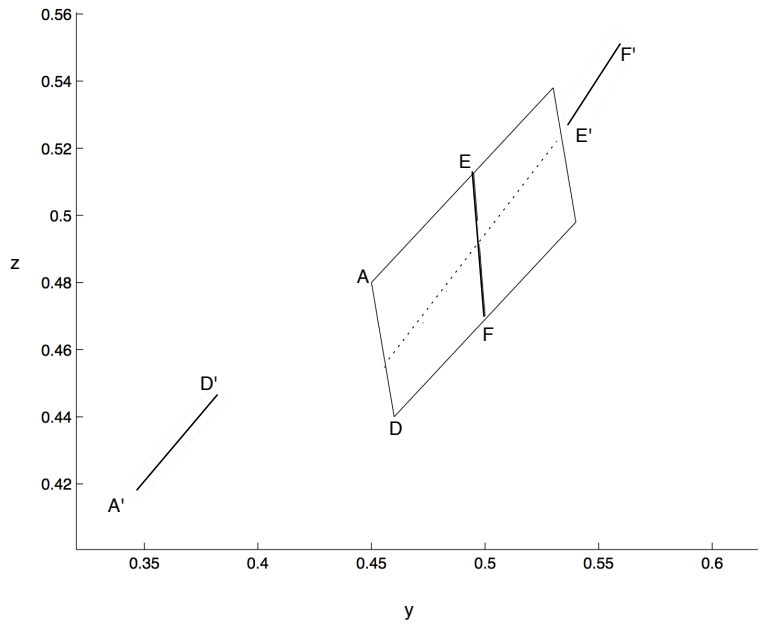

Figure 3.8: The image $|A'E'F'D'|$ of the quadrangle $|AEFD|$ under the map P.

Theorem 3.4.2. *The Poincaré map P corresponding to the Poincaré section $|\hat{A}\hat{B}\hat{C}\hat{D}|$ has the property that there is a closed invariant set $\hat{\Lambda} \subset |\hat{A}\hat{B}\hat{C}\hat{D}|$ for which $\hat{P}|\hat{\Lambda}$ is semi conjugate to the 2-shift map, Hence, $ent(\hat{P}) \geq \log 2 > 0$. This implies that attractor generated by system (3.4) with $a = 3.75, b = 0.7, c = 0.7, B = 2.5,$ has a positive topological entropy.*

Proof. In order to demonstrate the Theorem 6, two mutually disjointed subsets of $|\hat{A}\hat{B}\hat{C}\hat{D}|$ must be found, such that a $\hat{P}$-connected family with respect to them exists.

The subsets are denoted by Q_3 and Q_4 as shown in Fig. 3.10, the first subset Q_3 with the quadrangle $|\hat{A}\hat{D}\hat{E}\hat{F}|$. Under the first return Poincaré map $\hat{P}$, the subset Q_3 is mapped to $|\hat{A}'\hat{D}'\hat{E}'\hat{F}'|$ with $\hat{A}\hat{D}$ mapped to $\hat{A}'\hat{D}'$ and $\hat{E}\hat{F}$ mapped to $\hat{E}'\hat{F}'$. Again, the conclusion is the image $\hat{P}(Q_3)$ lies wholly across the quadrangle $|\hat{A}\hat{B}\hat{C}\hat{D}|$ with respect to $\hat{A}\hat{D}$ and $\hat{B}\hat{C}$ as shown in the Fig. 3.10.

The second subset Q_4 shown in , namely quadrangle $|\hat{G}\hat{B}\hat{C}\hat{H}|$, with $\hat{G}\hat{H}$ and $\hat{B}\hat{C}$ being its bottom and top edges, respectively. Like Q_3 the subset Q_4 is mapped

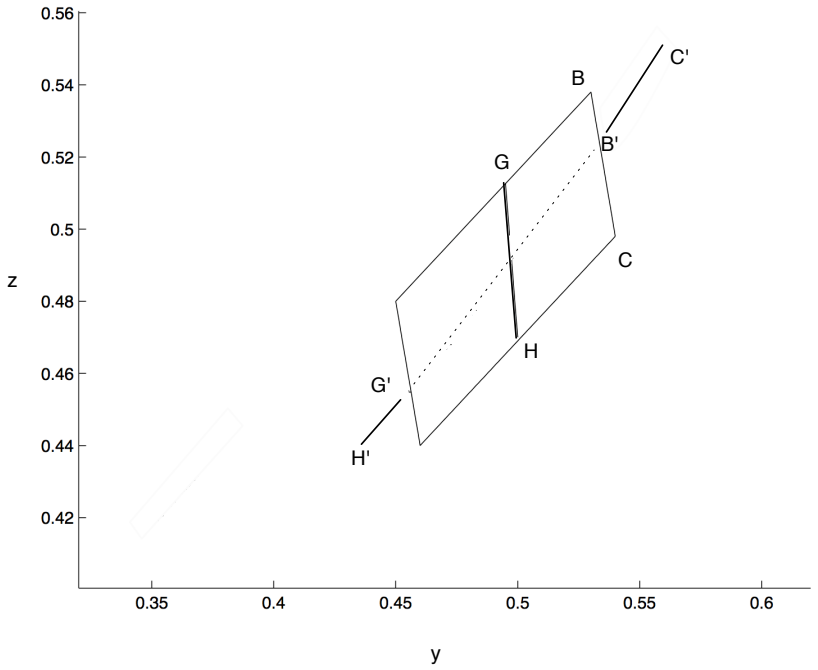

Figure 3.9: The image $|G'B'C'H'|$ of the quadrangle $|GBCH|$ under the map P.

to $|\hat{G}'\hat{B}'\hat{C}'\hat{H}'|$ under the Poincaré map $\hat{P}$ with $\hat{G}\hat{H}$ mapped to $\hat{G}'\hat{H}'$ and $\hat{B}\hat{C}$ mapped to $\hat{B}'\hat{C}'$. Thus, the image $\hat{P}(Q_4)$ lies wholly across the quadrangle $|\hat{A}\hat{B}\hat{C}\hat{D}|$ with respect to $\hat{A}\hat{D}$ and $\hat{B}\hat{C}$ as shown in the Fig. 3.11.

Evidently, the subsets Q_3 and Q_4 are mutually disjointed. Therefore, it follows that for every connection of $|\hat{A}\hat{B}\hat{C}\hat{D}|$ respect Q_3 and Q_4, for instance, Q_6, the images $\hat{P}(Q_6 \cap Q_3)$ and $\hat{P}(Q_6 \cap Q_4)$ also lie wholly across the quadrangle $|\hat{A}\hat{B}\hat{C}\hat{D}|$. Thus the images of $\hat{P}(Q_6 \cap Q_3)$ and $\hat{P}(Q_6 \cap Q_4)$ are still connections respect to Q_3 and Q_4.

According to Definition 2.3.1 and Theorem 2.3.3, there is a $\hat{P}$-connected family, so that the Poincaré map $\hat{P}$ is semi conjugate to the 2-shift map. Based on Theorem 2.3.4, it is concluded that the entropy of $\hat{P}$ is not less than $\log 2$, which implies that the attractor in Fig. 3.4 d) has a positive entropy. The proof is completed.

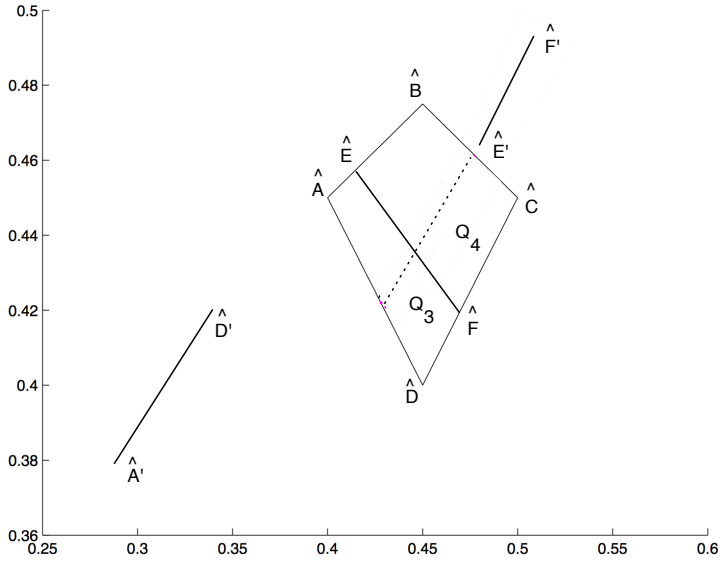

Figure 3.10: The image $|\hat{A}'\hat{E}'\hat{F}'\hat{D}'|$ of the quadrangle $|\hat{A}\hat{E}\hat{F}\hat{D}|$ under the map $\hat{P}$.

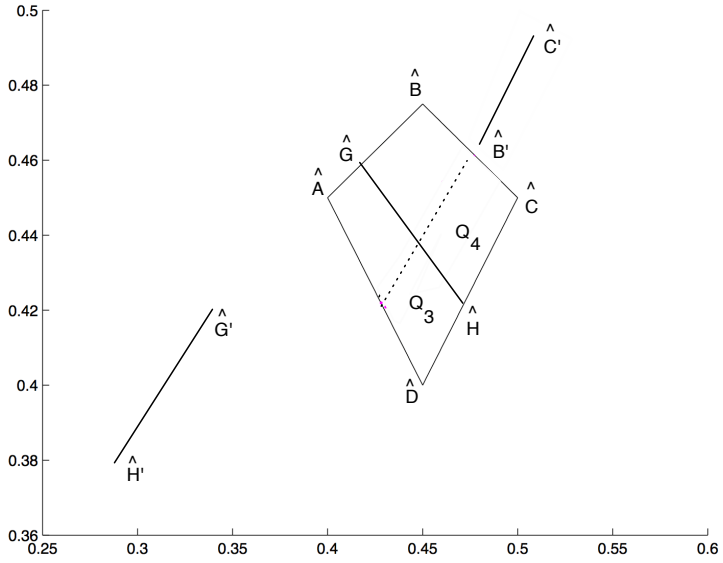

Figure 3.11: The image $|\hat{G}'\hat{B}'\hat{C}'\hat{H}'|$ of the quadrangle $|\hat{G}\hat{B}\hat{C}\hat{H}|$ under the map $\hat{P}$.

All these facts prove that the attractors of FOUDS with fractional orders 0.83, 0.82 and 0.8 are chaotic.

This section has studied the dynamics of a novel fractional order unstable dissipative system and has presented a computer-assisted proof for existence of horseshoe for Poincaré map derived from this system by virtue of topological horseshoe theory. The first return Poincaré map defined for the system is proved to be semi-conjugate to 2-shift map, and thus the system has a entropy no less than log 2, which obviously implies the system has chaotic dynamics.

Chapter 4

Electronic design of fractional order chaotic systems

From the mathematical model of a fractional order nonlinear system, the design of an electronic circuit, which is equivalent to the mathematical model, in the sense that it follows to the same set of equations is introduced. This section describes the design and simulation of an analog electronic circuit that realizes the fractional order unstable dissipative system with low orders i.e., the section gives the basic blocks needed for the realization of an electronic circuit equivalent to a fractional order nonlinear system. Where a synthesis approach to design the nonlinear function by using saturated functions, a rational approximation of fractional order operator is achieved, the rational approximation obtained is synthesized as an electronic ladder network called fractance device, which exhibits fractional order impedance properties.

4.1 Design of fractional order operators

In the literature about fractional order systems two approximating methods, time domain and frequency domain, have been implemented to compute the response of a fractional order systems numerically. The time domain methods are

based on the discretization of fractional-order differential equations. One of the best methods in this brach is an improved version of Adams-Bashforth-Moulton algorithm and is proposed based on the predictor-corrector scheme presented in above sections [32]. The frequency domain methods are based on fractional operator approximation. The frequency domain methods have been used to simulate the behavior of the chaotic fractional order systems [51–53]. Fractional order elements generally exhibit a constant phase curve, for that reason are also known as constant phase elements. In practice, a fractional order element can be approximated as a higher integer order system which maintains a constant phase within a chosen frequency band. To compute a solution of a fractional order system considering rational approximations of the fractional operators, first the fractional order equations of the system is considered in the frequency domain, and then Laplace transform of the fractional integral operator is replaced by its integer order approximation.

The fractional order elements can be rationalized by several iterative techniques namely, Charef's method [51], Carlson's method [52], Oustaloup's method [53], and among others. But one of the most common method to find rational approximation of the fractional operators is Charef method, due to the robustness gives an excelente relation between complexity and accuracy in the approximation. It is important to highlight the engagement between the error and complexity. The main idea is to find zeros and poles of a transfer function that has similar amplitude diagram as $1/s^{\alpha}$ in a given frequency range. The fractional operator $1/s^{\alpha}$ has a Bode amplitude diagram characterized by a slope of $-20\alpha\ dB/decade$. Therefore in this method, the $-20\alpha\ dB/decade$ line is approximated by a number of zigzag straight lines connected together with individuals slopes of $0\ dB/decade$ and $-20\ dB/decade$. According to this method, we can obtain a linear approximation of the fractional-order integrator with any desired accuracy over any frequency band. The order of this linear approximation system depends on the desired bandwidth and accuracy [54].

4.1.1 Fractional order integrator by Charef method

Fractional systems can be considered as a generalization of integer order systems. The most common instance of a fractional system transfer function is represented in the frequency domain by the following irrational transfer function

$$H(s) = \frac{1}{s^{\alpha}} \quad \alpha \in \mathbb{R}^{+} \tag{4.1}$$

which is called a fractional integrator and can be found in many physical phenomena, where $s = j\omega$ is the complex frequency and α is a positive real number such that $0 < \alpha < 1$. The fractional integrator may be approached by considering the basic formulation of Charef's approximation method, which is detailed in [51].

A system can be modeled in the frequency domain by the transfer function of a single fractional power pole as follows

$$H(s) = \frac{1}{(1 + s/p_T)^{\alpha}} \tag{4.2}$$

where p_T is the pole of the fractional order system and α is the fractional order of the system.

As shown in the Fig. 4.1, the slope with $-20\alpha\ dB/dec$ is estimated by a number of zigzag straight lines connected with individual slopes of $0\ dB/dec$ and $-20\ dB/dec$. The equation (4.2) can be rationalized by the following recursive formula

$$H(s) = \frac{\prod_{i=0}^{N-1}\left(1 + \frac{s}{z_i}\right)}{\prod_{i=0}^{N}\left(1 + \frac{s}{p_i}\right)}, \tag{4.3}$$

if a frequency range $\omega_{\max}$, a corner frequency p_T and the error y given in dB between the actual and approximate line are specified. Moreover, the zeros and poles can be recursively calculated as

$$\begin{aligned} z_{N-1} &= p_{N-1} 10^{[y/10(1-\alpha)]} \\ p_N &= z_{N-1} 10^{[y/10\alpha]}. \end{aligned} \tag{4.4}$$

The first approximation of the pole and zero is given by

$$\begin{aligned} p_0 &= p_T 10^{[y/20\alpha]} \\ z_0 &= p_0 10^{[y/10(1-\alpha)]} \end{aligned} \tag{4.5}$$

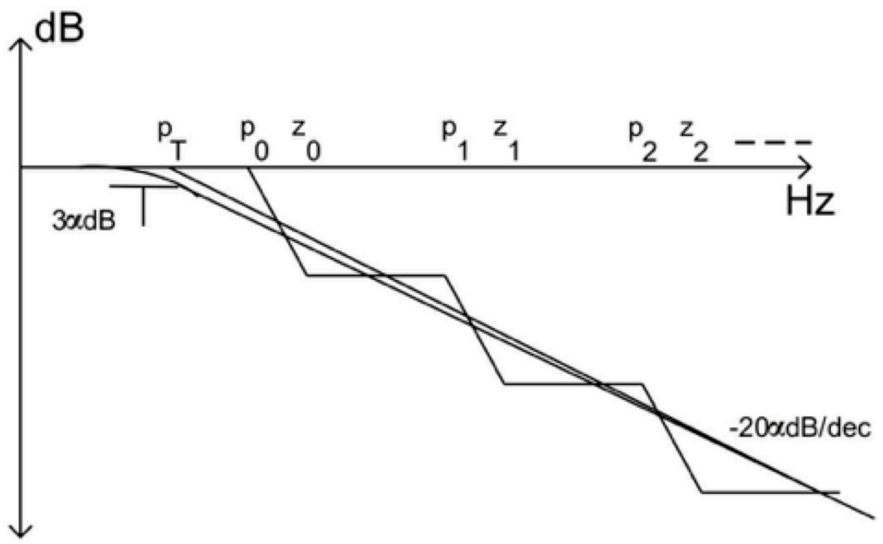

Figure 4.1: Bode plot with slope of $-20m\ dB/dec$ and its approximation with zigzag lines with individual slopes of $0\ dB/dec$ and $-20\ dB/dec$

The next step is to determine the value of N so that a specified accuracy of the approximated rational transfer function at the corner frequency can be obtained. The frequency corner p_T is determined in $-3\alpha\ dB$, p_0 is determined by the specified error, and p_N is determined by N, and a, b are given by

$$\begin{aligned} a &= 10^{[y/10(1-\alpha)]} = \frac{z_{N-1}}{p_{N-1}} \\ b &= 10^{[y/10\alpha]} = \frac{p_N}{z_{N-1}} \end{aligned} \tag{4.6}$$

where the location ratio of a zero to a previous pole is equal to the ratio of a pole to a previous zero, respectively, and it is equal to

$$ab = 10^{y/10\alpha(1-m)} = \frac{z_{N-1}}{z_{N-2}} = \frac{p_N}{p_N - 1}. \tag{4.7}$$

Now, N is determined by the following expression

$$N = \text{Integer}\left[\frac{\log\left(\frac{\omega_{max}}{p_0}\right)}{\log(ab)}\right] + 1. \tag{4.8}$$

4.1.2 Carlson's method

Fractional order elements or transfer functions can be recursively approximated considering the formulation known as Carlson's method [52], the idea is consider the newton process for approximate $(1/s)^{1/n}$, for any integer $n > 1$. The approximation is based on the algebraic expression $f(x) = x^n - a = 0$. The resulting approximation in real variables has the unique property of preserving upper ad lower approximation to the nth root of the real number a.

If $G(s)$ be a rational transfer function and $H(s)$ be a fractional order transfer function such that $H(s) = [G(s)]^q$ where $q = m/p$ is a fractional order of the transfer function, then $H(s)$ can be approximated as

$$H_i(s) = H_{i-1}(s)\frac{(p-m)[H_{i-1}(s)]^2 + (p+m)G(s)}{(p+m)[H_{i-1}(s)]^2 + (p-m)G(s)} \tag{4.9}$$

with an initial of $H_0(s) = 1$.

The recursive formula (4.9) can be written as

$$H_i(s) = H_{i-1}(s)\frac{G(s) + \alpha[H_{i-1}(s)]^2}{\alpha G(s) + [H_{i-1}(s)]^2} \tag{4.10}$$

where

$$\alpha = \frac{p-m}{p+m} = \left[\frac{1 - \left(\frac{m}{p}\right)}{1 + \left(\frac{m}{p}\right)}\right] \text{ and } \quad q = \frac{1-\alpha}{1+\alpha}. \tag{4.11}$$

Therefore, for the simple case i.e., $H(s) = s^q$, it will represent a differentiator for $q > 0$ consequently $\alpha < 1$. Also, it will act like an integrator for $q < 0$ implying $\alpha > 1$.

4.1.3 Oustaloup's method

Oustaloup's recursive filter gives a fitting to the fractional order elements s^γ within chosen frequency band [53]. Let us assume that the expected fitting range is (ω_b, ω_h). The filter can be written as

$$G_f(s) = s^\gamma = K \prod_{k=-N}^{N} \frac{s + \omega'_k}{s + \omega_k} \tag{4.12}$$

where the poles, zeros, and gain of the filter can be evaluated as

$$\omega_k = \omega_b \left(\frac{\omega_h}{\omega_b}\right)^{\frac{k+N+\frac{1}{2}(1+\gamma)}{2N+1}}, \quad \omega'_k = \omega_b \left(\frac{\omega_h}{\omega_b}\right)^{\frac{k+N+\frac{1}{2}(1-\gamma)}{2N+1}}, \quad K = \omega_h^{\gamma} \tag{4.13}$$

where N is order is the order of the finite transfer function approximation.

The approximation obtained by Charef Method shows that the overall process consists of a combination described by a single structure of pole-zero pair, this gives the fractional order factor in the log-log plot of the transfer function overall process.

4.2 Transfer function approximations

Employing the method given in section 4.1.1, where the purpose is approximate the system behavior in frequency domain. This is done for a given $0 < \alpha < 1$, i.e., by establish an approximation with bode magnitude response over the frequency band. The approximation is created by choosing an initial breaking point, an error in dB, and the number of poles in the approximation. The high frequency limit of the bandwidth can be varied by changing the allowable error and number of poles. Thus an approximation of any desired accuracy over any frequency band can be achieved. Table 4.1, gives the resulting approximations for transfer functions $H(s) = \frac{1}{s^{\alpha}}$ for different fractional orders, in increments of 0.1, assuming $\omega_{\max} = 10^3$ rad/s and $p_T = 1$. The maximum error 'y', considered in the computation an discrepancy error of $2\ dB$. According to this approach, is possible to obtain a linear approximation of the fractional order integrator with any accuracy and any frequency band. The order of this linear approximation system depends on the desired bandwidth and accuracy.

4.3 Fractance device

Until now we have understanding the capacitor with respect to considering the permittivity of the dielectric material. However, another possibility is to treat

Table 4.1: Integer order transfer functions approximations to fractional operators, with maximum discrepancy error $2\ dB$, and bandwidth of the system of $\omega_{\max}10^3$ rad/s.

		$H(s)$
$\frac{1}{s^{0.1}}$	$\approx$	$\frac{1000(s+16.6810)}{(s+10)(s+1.6681e3)}$
$\frac{1}{s^{0.2}}$	$\approx$	$\frac{3162(s+5.6234)(s+100)(s+1.7782e3)}{(s+3.1622)(s+56.2341)(s+1e3)(s+1.7782e4)}$
$\frac{1}{s^{0.3}}$	$\approx$	$\frac{1000(s+4.1595)(s+37.2759)(s+3.3404e2)(s+2.9935e3)}{(s+2.1544)(s+19.3069)(s+1.7301e2)(s+1.5505e3)(s+1.3894e4)}$
$\frac{1}{s^{0.4}}$	$\approx$	$\frac{177.82(s+3.8312)(s+26.1016)(s+177.8279)(s+1.2115e3)}{(s+1.7783)(s+12.1153)(s+82.5404)(s+562.3413)(s+3.8311e3)}$
$\frac{1}{s^{0.5}}$	$\approx$	$\frac{158.4893(s+3.9811)(s+25.1189)(s+158.4893)(s+1000)(s+6.3095e3)}{(s+1.5849)(s+10)(s+63.0957)(s+398.1072)(s+2.5119e3)(s+1.5849e4)}$
$\frac{1}{s^{0.6}}$	$\approx$	$\frac{31.6228(s+4.6416)(s+31.6228)(s+215.4435)(s+1.4678e3)}{(s+1.4678)(s+10)(s+68.1292)(s+464.1589)(s+3.1623e3)}$
$\frac{1}{s^{0.7}}$	$\approx$	$\frac{19.3070(s+6.4495)(s+57.7969)(s+517.9475)(s+4.6416e3)}{(s+1.3895)(s+12.4520)(s+111.5884)(s+1000)(s+8.9615e3)}$
$\frac{1}{s^{0.8}}$	$\approx$	$\frac{13.3352(s+13.335)(s+237.137)(s+4.217e3)(s+7.4989e4)}{(s+1.3335)(s+23.7137)(s+421.6965)(s+7.4989e3)(s+1.3335e5)}$
$\frac{1}{s^{0.9}}$	$\approx$	$\frac{3.5938(s+129.1550)(s+2.1544e4)}{(s+1.2915)(s+215.4435)(s+3.5938e4)}$

the device as an integrated system consisting of the dielectric and terminals, and further to only consider the relation between the current through and voltage drop cross entire system. This idea leads to consideration of Curie Law. The Curie suppose that the voltaje $v(t) = Vu(t)$ is applied to a capacitor possessing no initial stored charged. That is, there is no energy stored in the before applying the DC

voltage V. The current through the device will have the general form

$$i(t) = \frac{V}{ht^{\alpha}} \quad \text{for} \quad t > 0, \text{ and } 0 < \alpha < 1, \tag{4.14}$$

where h is a constant related to the capacitance and the kind of dielectric, and α is a constant related to the loss of capacitance. This is a power law dependence of terminal current upon the input voltage. The Laplace transform of the input voltage is

$$v(s) = \frac{V}{s}, \tag{4.15}$$

and the Laplace transform of $i(t)$ is

$$i(s) = \frac{\Gamma(1-\alpha)}{hs^{1-\alpha}} V, \tag{4.16}$$

where $\Gamma(\cdot)$ is the well known gamma function. Commonly, the impedance of a two terminal linear time invariant (LTI) circuit element is defined as

$$Z(s) = \frac{v(s)}{i(s)}, \tag{4.17}$$

The admittance is $Y(s) = 1/Z(s)$. From the Curie law device of (4.16) and (4.17) the next expression is obtained

$$Z(s) = \frac{h}{\Gamma(1-n)} \frac{1}{s^{\alpha}}, \tag{4.18}$$

of course, the ideal capacitor has impedance

$$Z(s) = \frac{1}{sC}. \tag{4.19}$$

The equation (4.18) is considered the fractional impedance, or fractance for short, is an electrical element which exhibits fractional order impedance properties. The impedance of the fractance device in the complex frequency domain is given by

$$Z(s) = as^{\alpha} \Rightarrow Z(j\omega) = a\omega^{\alpha} e^{j(\pi\alpha/2)} \tag{4.20}$$

where ω is the angular frequency, and α, for the special case of $\alpha = 1$ this element represents and inductor, for $\alpha = -1$ it represents a capacitor while for $\alpha = 0$

represents a resistance. In the range $-2 < \alpha < 0$ this element generally be considered to represent a fractional order capacitor. In the range $0 < \alpha < 2$ this element be considered to represent a fractional order inductor. At $\alpha = -2$, represents the frequency-dependent-negative-resistor [55].

A physical fractance device is not yet available in the form of a single commercial device. The fractance device can be emulated via higher order passive RC or RLC trees, chains or even a net grid type networks.

The fractance has many interesting properties. The phase angle is constant independent of the frequency, its magnitude versus frequency is nonlinear which can increase or decrease the effect of frequency for $\alpha > 1$ and $\alpha < 1$, that means it depends only on the value of fractional order α. The fractance is called as constant phase angle device of fractor. Moreover the extra parameter α added to the circuit design can be used further optimization, or design control. Furthermore by making the use of an operational amplifier, a fractional order differentiation and integration can be achieve.

The important point in the realization of fractance device is find the rational approximation of the fractional order operator. That is means, the design of fractance with order α can be done considering the rational approximations, then the values of the electrical elements, which are necessary for building a fractance are determined from the transfer functions obtained from the Charef approach.

4.4 Analog realization of fractional order circuits

In this section, the design electronic of a fractional order operator is synthesized for the fractance device, it has been presented in Fig 4.2, there are some different model as mentioned previously, some of the most commonly used are chain model and tree [16].

According to the circuit theory in the Laplace domain, the circuit between $n1$ and $n2$ nodes in Fig 4.2, can be used to realize the approximations of $\frac{1}{s^\alpha}$ with $0 < \alpha < 1$ in steps of 0.1 as shown in table 4.3 these transfer functions that approximate different fractional operators were computed considering the Charef

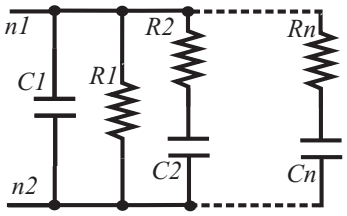

Figure 4.2: The circuit model of $\frac{1}{s^{\alpha}}$.

approach [51]. Now, according to the chapter 3 the system (3.4) does not show chaotic behavior for $\alpha < 0.9417$. However, in order to continue with the analyses and electronic implementation related to FOUDS, the fractional order $\alpha = 0.95$ is selected. In this case, to obtain a more accuracy approximation, hence, is selected the approximation error method given in [51] to be a 1dB. The approximation of $\frac{1}{s^{0.95}}$ with error of approximately is of 1dB and bandwith of 0.1rad/s to 1000rad/s is given by

$$\frac{1}{s^{0.95}} \approx \frac{1.16s^2 + 16.82s + 1.884}{s^3 + 18.4738s^2 + 2.6574s + 0.002976}. \tag{4.21}$$

In Fig 4.3, is displayed the Bode plot of the $1/s$ and the approximate transfer function. The bandwidth was considered in that sense to follow the operation regions where the operational amplifiers have a good behavior. As shown in the Fig. 4.3 the frequency response of the approximation function $\frac{1}{s^{0.95}}$ is almost superposed with the frequency response of $\frac{1}{s}$.

The corresponding circuit unit of (4.21) is displayed in Fig. 4.4 [56].

Using the circuit theory in the Laplace domain, is possible obtain the transfer function $H(s)$ between $n1$ and $n2$ in Fig. 4.4 as following

$$H(s) = R_1 || \frac{1}{sC_1} || \left(R_2 + \frac{1}{sC_2}\right) || \left(R_3 + \frac{1}{sC_3}\right) \tag{4.22}$$

$$= \frac{\frac{1}{C_0}\frac{C_0}{C_1}\left(s + \frac{1}{R_2C_2}\right)\left(s + \frac{1}{R_3C_3}\right)}{s^3 + \frac{(R_1C_1 + R_2C_2 + R_1C_2)R_3C_3 + R_1R_2C_2(C_1 + C_3)}{R_1R_2R_3C_1C_2C_3}s^2 + \frac{R_1C_1 + R_2C_2 + R_1C_2 + R_1C_3 + R_3C_3}{R_1R_2R_3C_1C_2C_3}s + \frac{1}{R_1R_2R_3C_1C_2C_3}},$$

where C_0 is the unit parameter. Letting $C_0 = 100\mu F$ and $F(s) = H(s)C_0 = \frac{1}{s^{0.95}}$ and comparing the equation (4.22) with equation (4.21) we can obtain the values of capacitances and resistances in Fig. 4.4 as follows: $C_1 = 86.20\mu F$, $C_2 = 29.85\mu F$,

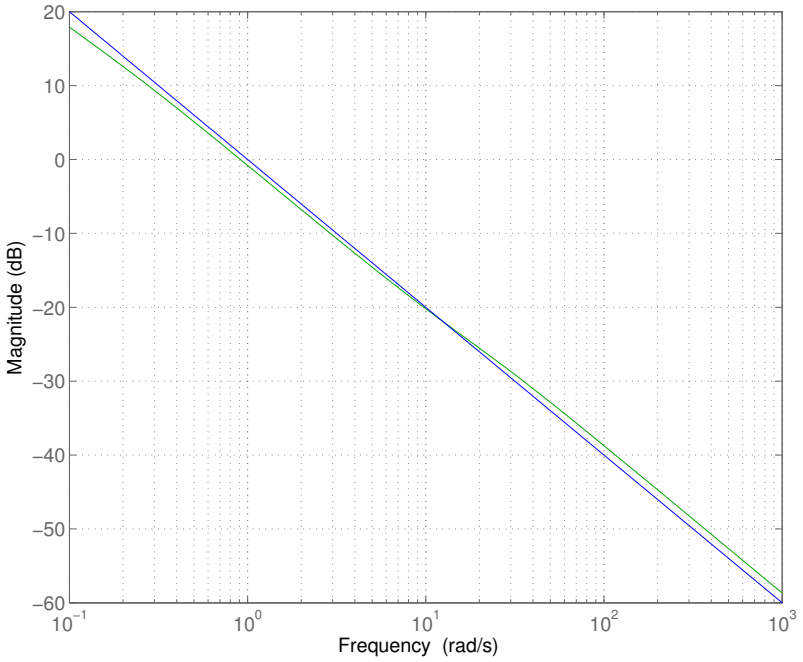

Figure 4.3: Bode plot of the approximate and the function of order $\alpha = 1$.

$C_3 = 23.56\mu F$, $R_1 = 6.28M\Omega$, $R_2 = .2966M\Omega$, and $R_3 = 2.945K\Omega$. Furthermore, in a similar sense, is possible to obtain the corresponding values of capacitances and resistances of the fractance device to realize $1/s^{\alpha}$ in Fig. 4.4.

To go on with the circuit design to realize the fractional order unstable dissipative system with $\alpha = 0.95$, is important to keep in mind that the design of a nonlinear function is an important part to generate chaotic attractors.

4.5 Synthesis of a nonlinear function

It is well known that a saturated circuit is one of the basic (piecewise linear) PWL circuits. The PWL model for nonlinear circuits is the operational amplifier (OPAMP). OPAMPs are electronic devices important for a wide range of applications. The PWL models that considering OPAMPs can be well characterized by

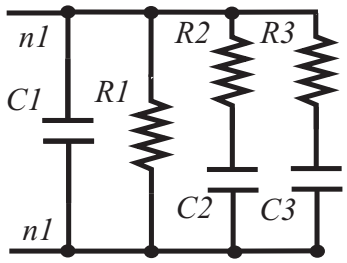

Figure 4.4: The circuit model of $\frac{1}{s^{0.95}}$.

saturated circuits. They are characterized by two differential inputs $V+$ and $V-$ and one output V_{out}. The transfer function characteristic of the opamp from input to output is PWL model and can be expressed as follows

$$V_{out} = f(v) = \begin{cases} -E_{sat} & \text{if } v \leq -\frac{E_{sat}}{A_v} \pm E, \\ Av & \text{if } -\frac{E_{sat}}{A} \pm E < v < \frac{E_{sat}}{A} \pm E, \\ E_{sat} & \text{if } v \geq \frac{E_{sat}}{A} \pm E. \end{cases} \tag{4.23}$$

Furthermore, saturated function working in voltage mode, where E_{sat} is the voltage value at which the output of the opamp saturates, moreover, depends on the internal circuitry design of the device and on the voltage supply applied. The region in which $V_{out} = Av$ is defined as the linear region, moreover E is the shifted voltage. Finally $v = V_- - V_+$ is the voltage between the two terminals V_- and V_+.

In the ideal case the operational amplifier can be characterized as follows:

- Infinite open loop gain and bandwidth
- Infinite common mode rejection ratio (CMRR)
- Infinite differential and common mode input resistance
- No noise and no feedback from the output to the input
- Negligible offset voltage and input current
- Zero output resistance

Real opamps posses finite values for these characteristics.

Based on the voltage saturated function, one can define the current saturated function as shown in [57] considering the Ohm law, the expression is given as

$$f(i) = \frac{f(v)}{R} \tag{4.24}$$

After of this consideration, one can realize the transformation between voltages saturated functions to current saturated functions. However, it is possible to get the saturated functions, which depend now on the opamp model [57].

$$V_{out} = \frac{A}{2}\left(\left|Vi + \frac{E_{sat}}{A} \pm E\right| - \left|Vi - \frac{E_{sat}}{A} \pm E\right|\right) \tag{4.25}$$

Henceforth, the parameters of the nonlinear function that is considered to generate the chaotic attractor defined in (3.4) are determined by (4.25) as shown in [57]. Where $k = E_{sat}$ is the saturated plateau, $sl = Vsat/\theta$ and $\theta = E_{sat}/A$ is the breaking point. The inverting configuration of the operational amplifier shown in Fig. 4.5a) is used to do the synthesis current saturated function of (4.25), moreover, the addition of a resistance R_{ia} in the out of the configuration is considered to enhance the voltage-to-current. The equations to design the nonlinear function are expressed as follows

$$k = RI_{sat}, \quad I_{sat} = \frac{V_{sat}}{R_{ia}}, \quad \theta = \frac{R_i|V_{sat}|}{R_f}, \quad s = \frac{k}{\theta}, \quad h = \frac{E}{\left(1 + \frac{R_i}{R_f}\right)} \tag{4.26}$$

By selecting $V_{sat} = \pm 8V$, $R = 10K\Omega$, $R_i = 1K\Omega$, $R_f = 1M\Omega$ and $R_{ia} = 64K\Omega$ and $E = 350mV$ in Fig. 4.6 the nonlinear function belongs to voltage and current are presented related to inverting configuration in Fig. 4.5. But a nonlinear function without the negative part is required to the design of fractional order unstable dissipative systems as shown in the equation (3.7). So a half wave rectifier is considered to do this operation, A simple method to do that is relating to add a pair of diode into the inverting configuration of the operational amplifier, as is displayed in the Fig. 4.7. In the output of this configuration is possible observe, that the current saturated function effectively has shifted in the current level, the Fig. 4.5b) presents the output related to voltage V_{in} against current Io.

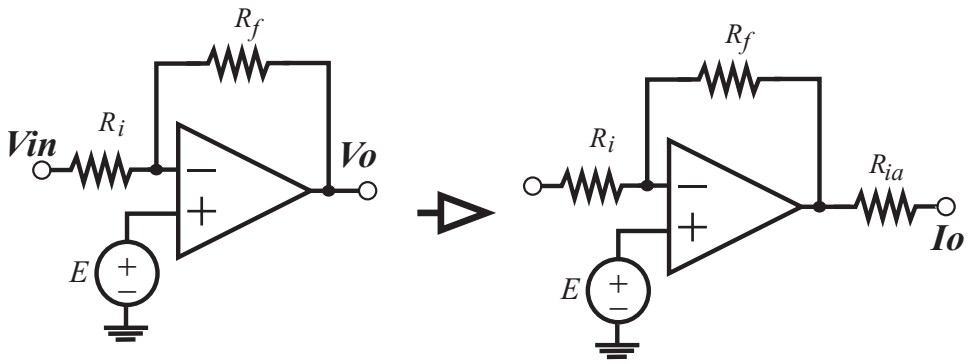

Figure 4.5: The inverting configuration of the operational amplifier to generate the nonlinear function.

4.6 Opamp-based fractional order unstable dissipative system

Now in this part of the design, considering the operational amplifiers, the fractance, the saturated current nonlinear function, resistors, and capacitors. The equivalent electronic circuit of (3.4) is designed, and then simulated with HSPICE (a circuit simulator) to verify that the behavior of the state variables are consistent with the numerical simulations analyzed before.

Starting from the circuit part associated to the first equation

$$D^{\alpha}x = y, \tag{4.27}$$

when $\alpha = 0.95$, the implementation of this equation needs one fractance integrator block to do the fractional order operator and an inverting configuration of the operational amplifier. Starting from this equation, it is possible to obtain the circuit scheme of Fig. 4.8. The synthesis obeys the equation

$$D^{\alpha}x = \frac{y}{R_{g1}C_0}, \tag{4.28}$$

In the similar way, it is possible to obtain the other two state variables remaining. The scheme circuit related to second equation is reported in Fig. 4.9 and the

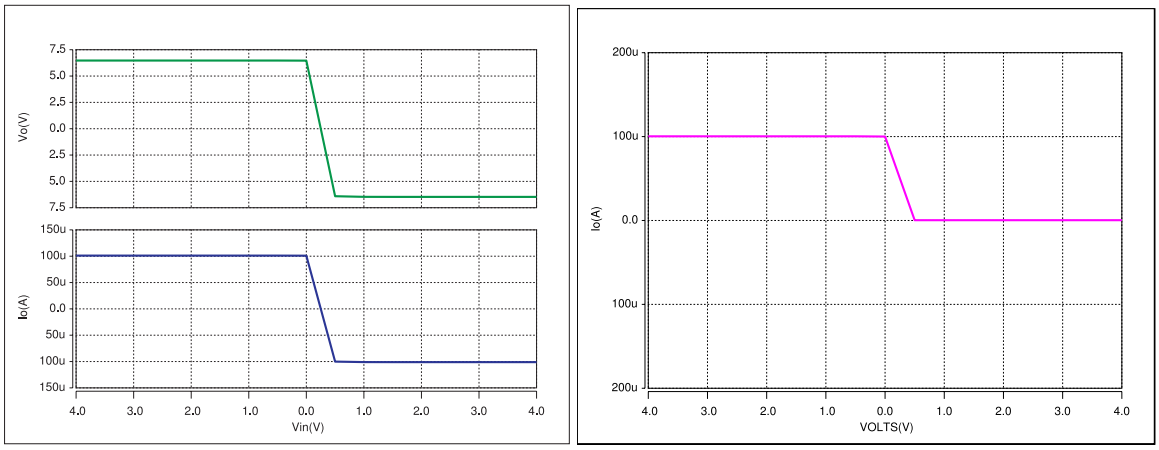

a) b)

Figure 4.6: The inverting configuration of the operational amplifier to generate the nonlinear function.

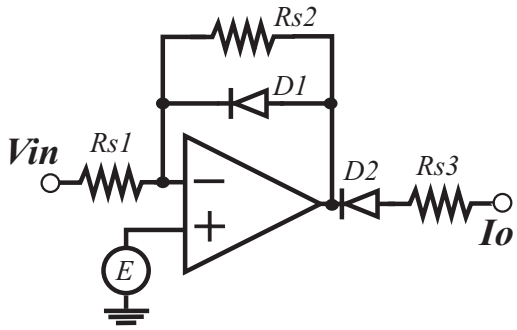

Figure 4.7: The inverting configuration of the operational amplifier to generate the nonlinear function considering a half wave rectifier.

associated equation as the following

$$D^{\alpha}y = \frac{y}{R_{g2}C_0} \tag{4.29}$$

Finally, the third equation is considered, in this equation one new type of term appear, and nonlinear function $g(x)$. To implement the term is realized through the saturated current nonlinear function as shown in Fig. 4.7, the third circuit equation is the following

$$D^{\alpha}z = -\frac{x}{R_xC_0} - \frac{y}{R_xC_0} - \frac{z}{R_xC_0} + \frac{i(x)R}{RC_0} \tag{4.30}$$

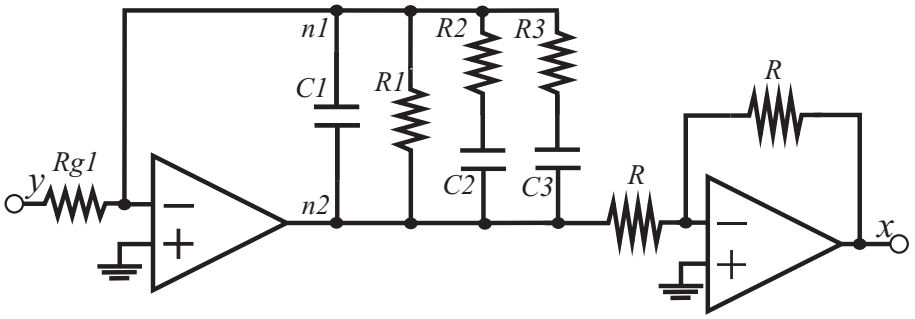

Figure 4.8: Scheme of the circuit related to the first fractional order unstable dissipative system. Parameters are: $C_1 = 86.20\mu F$, $C_2 = 29.85\mu F$, $C_3 = 23.56\mu F$, $R_1 = 6.28M\Omega$, $R_2 = 0.2966M\Omega$, and $R_3 = 2.945K\Omega$, $R_{g1} = R = 10K\Omega$.

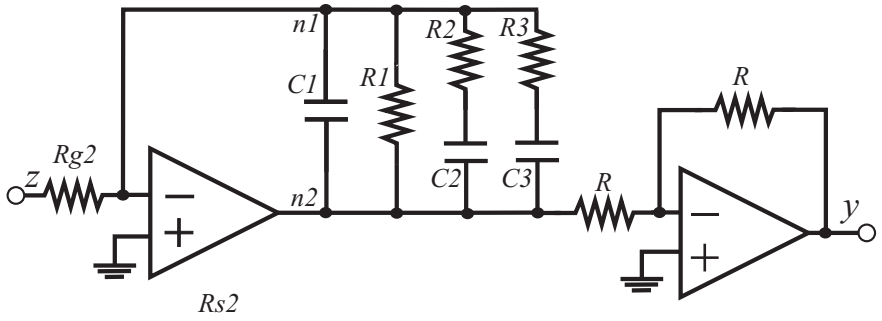

Figure 4.9: Scheme of the circuit related to the second fractional order unstable dissipative system. Parameters are: $C_1 = 86.20\mu F$, $C_2 = 29.85\mu F$, $C_3 = 23.56\mu F$, $R_1 = 6.28M\Omega$, $R_2 = 0.2966M\Omega$, and $R_3 = 2.945K\Omega$, $R_{g2} = R = 10K\Omega$.

From this equation, it is possible to obtain the circuit scheme of Fig. 4.10 and the parameters are determined by selecting a $C_0 = 100\mu F$

$$C_0 = \frac{1}{R}, \quad R_{g1} = R_{g2} = R_y = R_z = \frac{1}{C_0}, \quad R_x = \frac{1}{1.5C_0} \tag{4.31}$$

The whole circuit is obtained by assembling the three parts of Figs. 4.8, 4.9, 4.10, so that the electronic circuit equivalent to the fractional order unstable dissipative system is the circuit shown in Fig. 4.11 Once designed the fractional order unstable dissipative system to order $\alpha = 0.95$ it is checked through a circuit simulation tool HSPICE, to verify that the trends of state variables are in agreement with the theoretical analysis. By comparing the chaotic attractor in Fig. 4.12 with

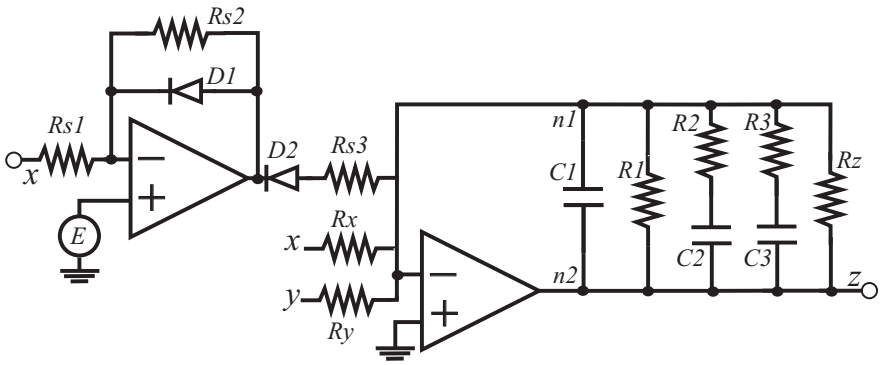

Figure 4.10: Scheme of the circuit related to the third fractional order unstable dissipative system. Parameters are: $C_1 = 86.20\mu F$, $C_2 = 29.85\mu F$, $C_3 = 23.56\mu F$, $R_1 = 6.28M\Omega$, $R_2 = 0.2966M\Omega$, $R_3 = 2.945K\Omega$, $R_y = R_z = R = 10K\Omega$, $R_x = 7.78K\Omega$, $R_{s1} = 1K\Omega$, $R_{s2} = 1M\Omega$, and $R_{s3} = 68K\Omega$, D1=D2=1n4001 and TL081 opamps.

the Fig. 3.3b). It can be concluded that the circuit simulations are consistent with the numerical simulations.

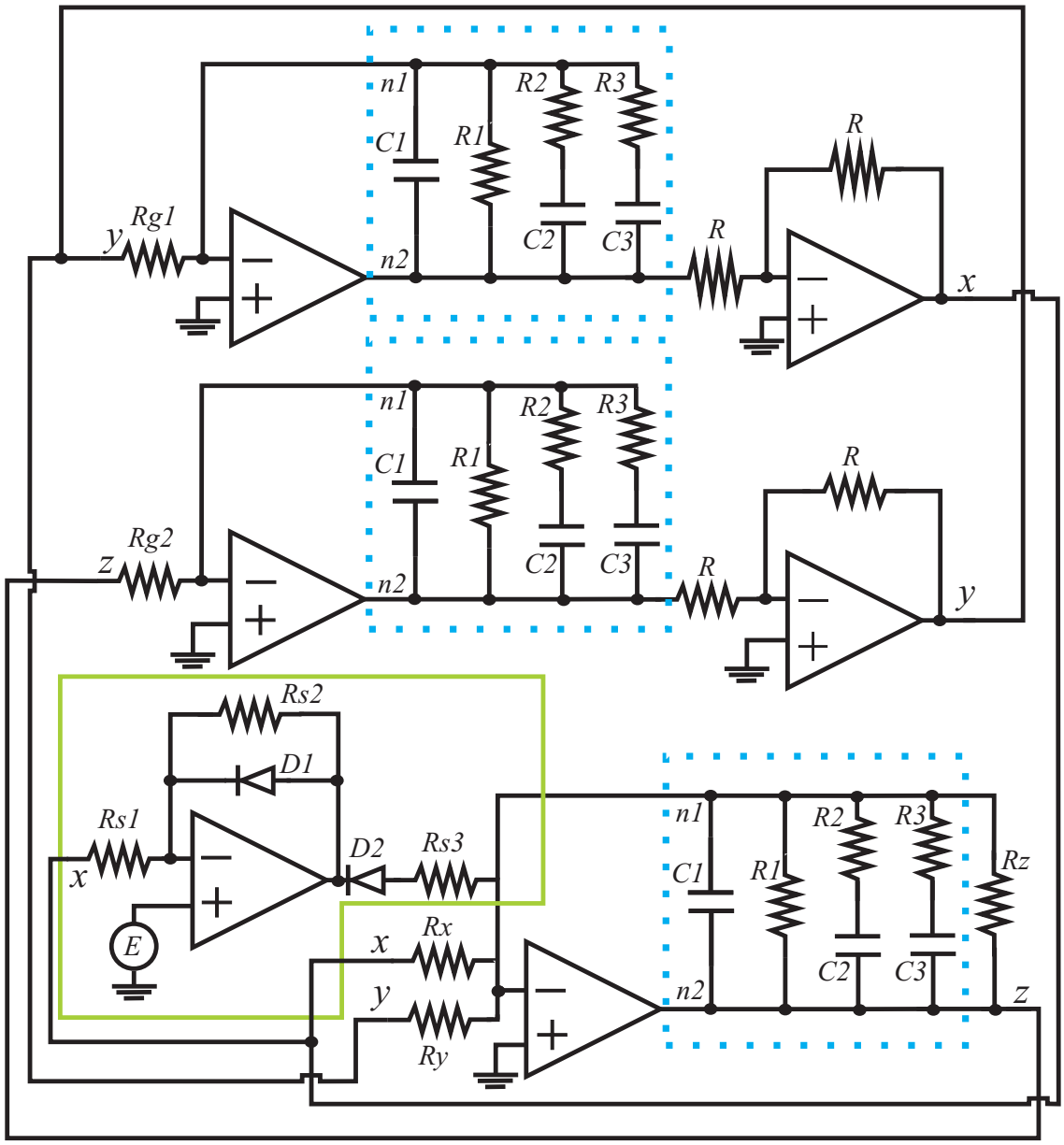

Figure 4.11: Scheme of the electronic circuit equivalent to the fractional order unstable dissipative system.

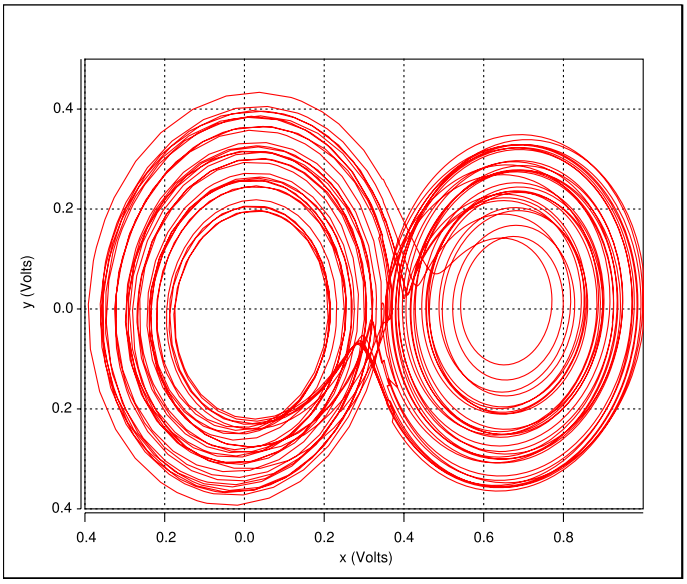

Figure 4.12: Circuit simulation of the chaotic attractor with fractional order $\alpha = 0.95$.

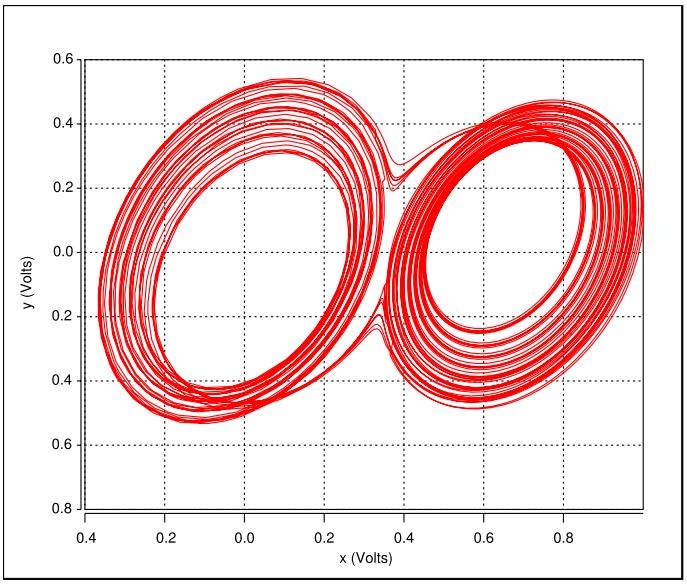

Figure 4.13: Circuit simulation of the chaotic attractor with fractional order $\alpha = 0.8$.

4.6.1 Opamp synthesis of lowest fractional order unstable dissipative system

Similarly, considering the system (3.4) with an order $\alpha = 0.8$, is now synthesized with opamps. Such system generates a chaotic attractor as shown in Fig. 3.4d). The difference with the design presented previously is the order of fractional order dynamical system and the values of its parameters. To build the analog circuit in first instance is necessarily consider a fractance that approximate the frequency response related to $\frac{1}{s^{0.8}}$. Selecting the integer order transfer function approximations to fractional operator of $\frac{1}{s^{0.8}}$ from the table 4.1. Using the circuit theory in the Laplace domain, it is possible to obtain the transfer function $H(s)$ between $n1$ and $n2$ in Fig. 4.2 as following.

$$H(s)=R_1||\frac{1}{sC_1}||\left(R_2+\frac{1}{sC_2}\right)||\left(R_3+\frac{1}{sC_3}\right)||\left(R_4+\frac{1}{sC_4}\right)||\left(R_5+\frac{1}{sC_5}\right) \quad (4.32)$$

where C_0 is the unit parameter. Letting $C_0 = 100\mu F$ and $F(s) = H(s)C_0 = \frac{1}{s^{0.95}}$ and comparing the equation (4.22) with equation (4.21) we can obtain the values of capacitances and resistances in Fig. 4.4 as follows: $C_1 = 0.1884\mu F$, $C_2 = 0.7619\mu F$, $C_3 = 0.6048\mu F$, $C_4 = 0.2545\mu F$, $C_3 = 0.1396\mu F$ $R_1 = 39.80M\Omega$, $R_2 = 9.839M\Omega$, and $R_3 = 0.9390M\Omega$, $R_4 = 0.09319M\Omega$, and $R_5 = 9.555K\Omega$. By changing the fractance obtained by the blue dotted box in the Fig. 4.12. The updated parameters are $Rx = 2.9K\Omega$, $Ry = Rz = 13.8K\Omega$, $R_{s3} = 25.37K\Omega$. In the Fig 4.13 displays the result of the circuit simulation done in HSPICE, to generate the chaotic attractor with two scrolls an lowest order.

In this chapter, the design of a fractional order unstable dissipative system with two different orders was presented, such as $\alpha = 0.95$ and $\alpha = 0.8$. Furthermore, based on frequency domain approximation a fractance device was considered to realize the fractional order operator, moreover, the nonlinear function was modeled by PWL approximation. It was shown that voltage saturated function can be synthesized with opamps and diodes by controlling the breakpoint and the vertical voltage shift.

Chapter 5

Conclusion

In this thesis, a fractional order unstable dissipative system has been introduced and analyzed, further, an electronic design of the system was developed. This chaotic system has abundant and complex dynamical behaviors. Dynamical behaviors of the system are analyzed, both theoretically and numerically, including some basic dynamical properties, as largest Lyapunov exponent, and so on.

First, the fundamentals definitions were presented about fractional calculus, furthermore, the state space representation of fractional order dynamical systems, a fundamental step to achieve the objective, moreover, the algorithm to compute the numerical solution of differential equations of fractional order, taking into account initial conditions was presented. The highlight of this algorithm is due to the fact that with the use of traditional integration methods it is impossible to obtain a solution, due these was done thinking in systems with integer order.

It was found that chaos exists in the fractional order three-dimensional system with its order as low as 2.4. By modifying the eigenvalues of the fractional system but preserving the same equilibrium points as interger-order case. The results have been validated by the existence of one positive Lyapunov exponent, and the topological horseshoe was found in order to confirm that the entropy of P is not less than $\log 2$. This proof guarantee that the proposed fractional order unstable dissipative system (FOUDS) can be generate chaotic behavior. In this way, the computer-assisted verification of chaos has been given by virtue of topological horseshoe theory, which is much more constructive and convincing than the usual method by calculating Lyapunov exponents. Such method is promising in rigorous

studies of chaos in the future, and can be used in estimating the topological entropy, proving the existence of chaos, showing the structure of chaotic attractors, revealing the mechanism inside of chaotic phenomena.

Furthermore, In order to investigate chaotic characteristics of fractional order unstable dissipative system, an analog circuit has been designed. Based on fractional frequency domain approximation and using integration circuit for the fractional order $\alpha = 0.95$ and $\alpha = 0.8$. Additionally, the synthesis of the block related to nonlinear function was built considering a half wave rectifier, the synthesis was realized taking into account a saturated function in current mode related to the state variable x. The results between numerical simulations and circuit simulations are in good agreement with each other, thus proving that chaos exists indeed in the proposed fractional order unstable dissipative system.

All these research results show that dynamics of the fractional order system are complex, which may provide a fractional system model for chaotic application, moreover the nonlinear electronic circuits is today of outstanding importance in the perspective of performing relevant topic, looking at analog circuit design as a fascinating scientific path.

Future work

The work reported opens the door to many interesting and novel directions of research. Building on the top of the results, more features can be added to increase the chaotic behavior of the fractional order system. So, some of the worth mentioning extensions are outlined as follows:

- Enriching the dynamics of the proposed system, including more switching functions to generate two-directional and three-directional multiscroll fractional order chaotic systems.
- Propose a scheme of synchronization to fractional order unstable dissipative system.
- The design of fractional order unstable dissipative system, was proposed

considering analog electronic components, so a digital implementation of this systems considering embedded systems is a next step due to their applications in modern digital systems.

- Consider the Adomian decomposition method, which provides series solutions that converge rapidly. It is free from rounding off errors. To a new representation of fractional order unstable dissipative system.

Appendix A

In this appendix, the results of this thesis are reported in the following articles, these have been presented in international conferences and published in journals belong to the journal citation report (JCR).

E. Zambrano-Serrano, J.M. Muñoz-Pacheco and E. Campos-Cantón. Chaos generation in fractional-order switched systems and its digital implementation, *AEÜ - International Journal of Electronics and Communications* accepted may 2017.

E. Zambrano-Serrano, J.M. Muñoz-Pacheco and E. Campos-Cantón. Circuit synthesis of an incommensurate fractional order multi-scroll PWL chaotic system. *6th International Conference on Modern Circuits and Systems Technologies (MOCAST)*. May. 2017.

E. Zambrano-Serrano, E. Campos-Cantón and J.M. Muñoz-Pacheco. Strange attractors generated by a fractional order switching system and its topological horseshoe. *Nonlinear Dynamics*. 83(3): 1629-1641, Oct. 2015.

E. Zambrano-Serrano, J.M. Muñoz-Pacheco and E. Campos-Cantón. Opamp-based synthesis of a fractional order switched system. *5th International Conference on Modern Circuits and Systems Technologies (MOCAST)*. May. 2016.

E. Zambrano-Serrano. Chaotic oscillator derived from a fractional order dynamic system. *2015 Workshop on chaotic and nonlinear dynamics in circuits and*

Systems. Dec. 2016

Appendix B

In this appendix the pseudocode related to algorithm predictor-corrector from the Chapter 1 is presented.

Input Variables

f the real-valued function that defines the right-hand side of the fractional differential equation

α order of the differential equation (a positive number between 0 and 1)

y_0 an array of real numbers that contains the initial conditions

T the upper bound of the interval where the solution is to be approximated

T_0 The lower bound of the interval where the solution is to be approximated

h the time step integration

Output Variables

y an array of $m \times N + 1$ real numbers that contains the approximate solutions

t an array of $N + 1$ real numbers that contains the time solution from T_0 until T with increase of h

Internal Variables

m the number of initial conditions

N the number of time steps that the algorithm is to consider

i, j variables used as indices

a, b arrays of $m \times N + 1$ real numbers that contain the values of the corrector and predictor, respectively

p the predicted value

Body of the Method

$N = floor((T - T_0)/h)$
$m = length(y_0)$
$y = zeros(m, N)$
for $j = 1$ to N
    $b[1, j] = j^\alpha - (j-1)^\alpha$
    $a[1, j] = (j+1)^{\alpha+1} - 2j^{\alpha+1} + (j-1)^{\alpha+1}$
end
$y(:, 1) = y_0$
for $i = 1$ to N
    $p = y(:, i) + \frac{h^\alpha}{\Gamma(\alpha+1)} \sum_{i=1}^{j} b[i] f(ih, y(i))$
    $y(:, i+1) = y(:, i) + \frac{h^\alpha}{\Gamma(\alpha+2)} \left(f(ih, p) + ((i - 1 - \alpha) i^{j^\alpha}) f(0, y[0]) + \sum_{i=1}^{i} a[i] f(ih, y[i]) \right)$
end

Bibliography

[1] S. G. Samko, A. A. Kilbas, and O. I. Marichev. *Fractional Integrals and Derivatives*. Gordon and Breach Science Publishers, Amsterdam, 1993.

[2] K. S Miller and B. Ross. *An Introduction to the Fractional An Introduction to the Fractional Calculus and Fractional Differential Equations*. John Willey & Sons Ltd., Publication, New York, NY, USA, 1993.

[3] E. Capelas de Oliveira and J. A. Tenreiro-Machado. A review of definitions for fractional derivatives and integral. *Mathematical Problems in Engineering*, 2014:1–6, 2014.

[4] Y. Zhou. *Basic Theory of Fractional Differential Equations*. World Scientific Publishing, Hackensack, NJ, USA, 2014.

[5] K. B. Oldham and J. Spanier. *The Fractional Calculus, Theory and Applications of Differentiation and Integration to Arbitrary Order*. Dover Publications, Inc., 2002.

[6] K. Diethelm. *The Analysis of Fractional Differential Equations: An Application-Oriented Exposition Using Differential Operators of Caputo Type*, volume 2004 of *Lecture Notes in Mathematics*. Springer Berlin Heidelberg, Germany, 2010.

[7] R. Gorenflo and F. Mainardi. *Fractals and Fractional Calculus in Continuum Mechanics*, volume 378 of *Courses and Lectures*. Springer Vienna, Wien, 1997.

[8] Y. Zhou, C. Ionescu, and J. A. Tenreiro-Machado. Fractional dynamics and its applications. *Nonlinear Dyn.*, 80(4):1661–1664, Jun. 2015.

[9] S. Abbas, M. Benchohra, and G. M. N'Guerekata. *Topics in Fractional Differential Equations*, volume 27 of *Developments in Mathematics*. Springer New York, London, 2012.

[10] S.A. David, J. A. Tenreiro-Machado, D. D. Quintino, and J. M. Balthazar. Partial chaos suppression in a fractional order macroeconomic model. *Mathematics and Computers in Simulation*, 122:55–68, Apr. 2016.

[11] M. D. Ortigueira and J. A. Tenreiro-Machado. What is a fractional derivative? *Journal of Computational Physics*, 293:4–13, Jul. 2015.

[12] C. Ionescu. A memory-based model for blood viscosity. *Commun. Nonlinear Sci. Numer. Simulat.*, 45:29–34, Sep. 2017.

[13] R. Metzler and J. Klafter. The random walk's guide to anomalous diffusion: a fractional dynamics approach. *Physics Reports*, 339(1):1–77, Dec. 2000.

[14] A. Ebaid. Analysis of projectile motion in view of fractional calculus. *Applied Mathematical Modelling*, 35(3):1231–1239, Mar. 2011.

[15] R. Caponetto, G. Dongola, L. Fortuna, and I. Petras. *Fractional Order Systems Modeling and Control Applications*, volume 72 of *A*. World Scientific Publishing, 2010.

[16] I. Podlubny. *Fractional Differential Equations Mathematics in Science and Engineering*, volume 198. Academic Press, New York, 1999.

[17] C. A. Monje, Y. Chen, B. M. Vinagre, D. Xue, and Vicente Feliu. *Fractional-Order Systems and Controls Fundamentals and Applications*. Springer-Verlag London Limited, London, 2010.

[18] I. Petras. *Fractional-Order Nonlinear Systems Modeling, Analysis and Simulation*. Higher Education Press, Berlin, 2011.

[19] S. Arshad, A. Sohail, and S. Javed. Dynamical study of fractional order tumor model. *Int. J. Bifurc. Chaos*, 12(5):1550032 1–12, May. 2015.

[20] Q. Xu, M. Shi, and Z. Wang. Stability and delay sensitivity of neutral fractional-delay systems. *Chaos*, 26(8):084301 1–10, Aug. 2016.

[21] M. S. Tavazoei, M. Haeri, S. Jafari, S. Bolouki, and M. Siami. Some applications of fractional calculus in suppression of chaotic oscillations. *IEEE Trans. Industrial Electronics*, 55(11):4094–4101, Nov. 2008.

[22] A. Sasso, G. Ducharne, and G. Palmieri. Application of fractional derivative models in linear viscoelastic problems. *Mech. Time Depend Mater.*, 15:367–387, Sep. 2011.

[23] B. Li and W. Xie. Image denoising and enhancement based on adaptive fractional calculus of small probability strategy. *Neurocomputing*, 175:704–714, Oct. 2015.

[24] D. Guyomar, B. Ducharne, G. Sebald, and D. Audiger. Fractional derivative operators for modeling the dynamic polarization behavior as a function of frequency and electric field amplitude. *IEEE Trans. Ultrason. Ferroelectr. Freq. Control*, 56(3):437–443, Mar. 2009.

[25] A. Kiani-B, K. Fallahi, N. Pariz., and H. Leung. A chaotic secure communication scheme using fractional chaotic systems based on an extended fractional kalman filter. *Commun. Nonlinear Sci.*, 14(3):863–879, Mar. 2009.

[26] P. Muthukumar, P. Balasubramaniam, and K. Ratnavelu. Fast projective synchronization of fractional order chaotic and reverse chaotic systems with its application to an affine cipher using date of birth (dob). *Nonlinear Dyn.*, 80(4):1883–1897, Jun. 2015.

[27] Y. Luo and YQ. Chen. *Fractional Order Motion Controls*. John Willey & Sons, Ltd., Publication, United Kingdom, 2013.

[28] C. Yang and F. Liu. A computationally effective predictor-corrector method for simulating fractional order dynamical control system. In Andrew Stacey, Bill Blyth, John Shepherd, and A. J. Roberts, editors, *Proceedings of the 7th Biennial Engineering Mathematics and Applications Conference, EMAC-2005*, volume 47 of *ANZIAM J.*, pages C168–C184, Aug. 2006.

[29] Y. Luchko and R. Gorenflo. An operational method for solving fractional differential equations with the caputo derivatives. *Acta Mathematica Vietnamica*, 24(2):207–233, 1999.

[30] D. Matignon. Generalized fractional differential and difference equations: Stability properties and modelling issues. In *Proceedings of Math. Theory of Networks and Systems Symposium*, Padova, Italy, 1998.

[31] D. Matignon. Stability result on fractional differential equations with applications to control processing. In *Proceedings IMACS-SMC*, pages 963–968, Lille, France, 1996.

[32] K. Diethelm, N. J. Ford, and A. D. Freed. A predictor-corrector approach for the numerical solution of fractional differential equations. *Nonlinear Dyn.*, 29(1):3–22, Jul. 2002.

[33] J. M. Muñoz-Pacheco, E. Zambrano-Serrano, O. Félix-Beltrán, L. C. Gómez-Pavón, and A. Luis-Ramos. Synchronization of pwl function-based 2d and 3d multi-scroll chaotic systems. *Nonlinear Dyn.*, 70(2):1633–1643, Aug. 2012.

[34] E. Tlelo-Cuautle and J. M. Muñoz-Pacheco. Simulation of chua's circuit by automatic control of step-size simulation of chua's circuit by automatic control of step-size simulation of chua's circuit by automatic control of step-size. *Appl. Math. Comput.*, 190(2):1526–1533, Jul. 2007.

[35] G. C. Layek. *An Introduction to Dynamical Systems and Chaos*. Springer Berlin Heidelberg, New York, NY, USA, 2015.

[36] J. L. Moiola and G. Chen. *Hopf Bifurcation Analysis: A Frequency Domain Approach*. World Scientific Publishing, 1996.

[37] C. Li and Y. Ma. Fractional dynamical system and its linearization theorem. *Nonlinear Dyn.*, 71(4):621–633, 2013.

[38] T. S. Parker and L. O. Chua. *Practical Numerical Algorithms for Chaotic Systems*. Springer-Verlag, New York, 1989.

[39] S. Wiggins. *Introduction to Applied Nonlinear Dynamical Systems and Chaos*. Texts in Applied Mathematics. Springer-Verlag, New York, 2003.

[40] J. Guckenheimer and P. Holmes. *Nonlinear Oscillations, Dynamical Systems, and Bifurcations of Vector Fields*. Applied Mathematical Sciences. Springer Science+Business Media, New York, 1983.

[41] X. Yang. Topological horseshoes and computer assisted verification of chaotic dynamics. *Int. J. Bifurc. Chaos*, 19(4):1127–1145, Apr. 2009.

[42] W. Wu, Z. Chen, and Z. Yuan. A computer-assisted proof for the existence of horseshoe in a novel chaotic system. *Chaos Soliton Fractals*, 41(5):2756–2761, Sep. 2009.

[43] X. Yang, Y. Yu, and S. Zhang. A new proof for existence of horseshoe in the rössler system. *Chaos Soliton Fractals*, 18(2):223–227, Oct. 2003.

[44] X. Yang and Y. Tang. Horseshoes in piecewise continuous maps. *Chaos Soliton Fractals*, 19(4):841–845, Mar. 2004.

[45] T. L. Devaney. *An Introduction to Chaotic Dynamical Systems*. Studies in Nonlinearity. Westview Press, 2003.

[46] E. Campos-Cantón, J. G. Barajas-Ramirez, G. Solis-Perales, and R. Femat. Multiscroll attractors by switching systems. *Chaos*, 20(1):1–6, Mar. 2010.

[47] E. Campos-Cantón. Switched systems based on unstable dissipative systems dissipative systems. In *IFAC-PapersOnLine*, volume 48, pages 116–121, Tokio, Japan, Aug. 2015. Elsevier Ltd.

[48] R. Hegger, H. Kantz, and T. Schreiber. Practical implementation of nonlinear time series methods: the tisean package. *Chaos*, 9:413–435, 1999.

[49] Q. Li and X. Yang. A 3d smale horseshoe in a hyperchaotic discrete-time system. *Discrete Dynamics in Nature and Society*, 2007:1–9, Nov. 2007.

[50] J. Kennedy and J. A. Yorke. Topological horseshoes. *Transactions American Mathematical Society*, 353(6):2513–2530, Feb. 2001.

[51] A. Charef, H. H. Sun, Y. Y. Tsao, and B. Onaral. Fractal system as represented by singularity function. *IEEE Trans. Autom. Control*, 37(9):1465–1470, Nov. 1992.

[52] G. Carlson and C. Halijak. Approximation of fractional capacitors $(\frac{1}{s})^{\frac{1}{n}}$ by a regular newton process. *IEEE Trans. Circuits Theory*, 11(2):210–213, Jun. 1964.

[53] A. Oustaloup, F. Levron, B. Mathieu, and F. M. Nanot. Frequency-band complex noninteger differentiator: characterization and synthesis. *IEEE Trans. Circuits Syst. I Fundam. Theory Appl.*, 47(1):25–39, Jan. 2000.

[54] M. S. Tavazoei and M. Haeri. Unreliability of frequency-domain approximation in recognising chaos in fractional-order systems. *IET Signal Processing*, 1(4):171–181, Jan. 2008.

[55] A. G. Radwan, A. M. Soliman, and A. S. Elwakil. First-order filters generalized to the fractional domian. *J. Circuit Syst. Comp.*, 17(1):55–66, Feb. 2008.

[56] Z. Ruo-Xun and Y. Shi-Ping. Chaos in fractional-order generalized lorenz system and its synchronization circuit simulation. *Chinise Physics B*, 18(8):3291–3303, Aug. 2009.

[57] J. M. Muñoz-Pacheco and E. Tlelo-Cuautle. *Electronic Design Automation of Multi-Scroll Chaos Generators*. Bentham Science Publishers, 2010.